PERGAMON

International Journal of Solids and Structures 36 (1999) 1883–1923

INTERNATIONAL JOURNAL OF SOLIDS and STRUCTURES

# Hybrid finite element formulations for elastodynamic analysis in the frequency domain

J. A. Teixeira de Freitas

*Departamento de Engenharia Civil, Instituto Superior Técnico, Av. Rovisco Pais, 1096 Lisboa Codex, Portugal*

Received 4 December 1995; in revised form 16 February 1998

**Abstract**

Three alternative sets of hybrid formulations to solve linear elastodynamic problems by the finite element method are presented. They are termed hybrid–mixed, hybrid and hybrid–Trefftz and differ essentially on the field conditions that the approximation functions are constrained to satisfy locally. Two models, namely the displacement and the stress models, are obtained for each formulation depending on whether the tractions or the boundary displacements are the field chosen to implement interelement continuity. A Fourier time discretization is used to uncouple the solving system in the frequency domain. The basic space discretization criterion is implemented directly on the fundamental relations of elastodynamics and used to derive the stress and displacement models of the hybrid–mixed formulation. The hybrid and hybrid–Trefftz formulations are presented in sequence as the variants of the hybrid–mixed formulation obtained by progressively increasing the constraints on the approximation bases. Numerical implementation aspects are briefly discussed and the performance of the finite element models is illustrated with numerical applications. 

*Keywords:* Hybrid finite elements; Elastodynamics; Spectral analysis

## 1. Introduction

The objective of this paper is to present a coherent set of hybrid finite element formulations for structural dynamics, ranging and relating directly to the hybrid–mixed, the hybrid and the hybrid–Trefftz approaches. As in the conventional approach, two basic finite element models are distinguished in each formulation, namely the displacement and the stress models.

As every other hybrid variant of the finite element method reported in the literature, the models and formulations analysed here may also be directly related with the pioneering work of de Veubeke (1965) and Pian and Tong (1969). What distinguishes the results to be presented are specific steps and techniques adopted in the derivation of the alternative hybrid finite element models and formulations, which root directly in the mesh and nodal formulations

0020–7683/99/$ - see front matter 
PII: S0020–7683(98)00064–X

proposed by Munro and Smith (1972) in the context of skeletal structures, see Freitas (1989).

The hybrid–Trefftz stress and displacement models presented here related directly with the HT-D and HT-T elements developed by Jirousek and his co-workers, see Jirousek and Wróblewski (1996) for a state of the art review on this subject. Despite the distraction and confusion they may cause, the different designations used here (namely HT-S and HT-D) are retained to emphasise the direct relationship of the hybrid–Trefftz stress and displacement models with the corresponding models of the hybrid–mixed and hybrid formulations.

From a formal standpoint, the main contribution of the work being presented is to establish the direct linkage that exists between these formulations and to identify in a clear way the distinguishing features of the displacement and stress models. It is also instrumental to challenge the concept that the three sets of formulations are independent and unrelated, and to support the proper classification of some of the models presented in the literature, namely the HT-D and HT-T variants of the T-elements, which are stress and displacement elements, respectively, and not the inverse as viewed by some authors.

In terms of content, the distinguishing feature shared by all formulations and models discussed here is the extensive use of generalized variables, in detriment of nodal variables. The overuse of the node concept has hindered the development of the hybrid formulations, and of the stress model in particular, and has also discouraged the research on $p$-adaptive processes. As the formulations and models being presented are naturally hierarchical and based on strongly localised (generalised) variables, they may motivate the reinvestment in $p$-adaptivity, specially at a moment when so much work is being devoted to parallel processing.

Moreover, all formulations and models may incorporate easily the simulation of local effects, in particular those associated with singular stress fields or with localised deformations. This possibility weakens what is perhaps the strongest argument used so far to justify the investment made in the alternative $h$-adaptive processes: the inability of $p$-adaptivity to model conveniently such effects.

The only effective way of fulfilling the objective of confronting and relating directly the hybrid variants is to embrace in the same text the three alternative formulations and the two alternative models. The layout of the paper is designed to minimise the consequent risk of producing a too cumbersome and insufficiently clear presentation.

Hence, the presentation starts with a brief description of the approach followed in the derivation of hybrid elements, which is used to stress the main features and weakness of each variant. The derivation procedure is then applied, step by step, for each formulation and model. The more general hybrid–mixed formulation is derived first and the hybrid and hybrid–Trefftz formulations are presented in a sequence designed to emphasise that they correspond to particular cases characterised by a progressive constraining of the approximation bases.

To focus on the essential aspects that relate and distinguish these formulations and models, they are established for the basic linear elastodynamic problem, to be solved in the frequency domain. Also, and following valuable suggestions by the reviewers, immediately non-essential information is relegated to the appendices to the main text.

## 2. Derivation of hybrid elements

The ultimate target in the development of the displacement model is to generate kinematically admissible solutions and it relates directly with the conventional displacement or conforming finite

element model. As for the conventional equilibrium finite elements, the alternative stress model is designed to produce statically admissible solutions.

Independently of the model being developed, different levels in the constraining of the finite element approximation basis can be stated a priori. Three levels are considered here, leading to the alternative hybrid–mixed, hybrid and hybrid–Trefftz formulations. Each of these formulations is written for both the stress and the displacement models, leading to a set of six forms for encoding the linear elastodynamic problems under consideration.

### 2.1. Fundamental relations

Most hybrid and mixed variants of the finite element method are derived either from well established or newly coined variational statements or from the equivalent boundary value problem. In the present context, this is the wave equation and the constraining initial, Dirichlet and Neumann conditions, written in terms of the displacement field and its time and space gradients.

To identify clearly the approximations made and how the different equations are enforced, the finite element model is derived here not directly from the wave equation but explicitly from the supporting equilibrium, compatibility and elasticity conditions.

An added advantage of this approach is to produce finite element equilibrium and compatibility equations that are independent of the local constitutive relations and obtain a finite element description of the constitutive relations that does not depend on the local static and kinematic admissibility conditions. The modular nature of the finite element models and formulations thus derived enhances their generalisation to physically or geometrically non-linear problems.

### 2.2. Time and space distribution

After stating the fundamental relations governing the problem under analysis, the next step in the derivation presented below addresses the criteria for time and space discretization. The solution space is constrained by the usual separation of variables in time and space and, as it is typical of the method of spectral analysis, in the ensuing discretization of the time domain a Fourier expansion is enforced to uncouple the fundamental relations in a sequence of problems in the frequency domain.

Space discretization is so addressed as to fully exploit the freedom offered by the mixed approach of the finite element method. In the present context of elastic analysis, this means the possibility of approximating independently two fields in the domain of the element, the stresses and the displacements (and thus the mixed label), and one field on its boundary, either the tractions or the displacements (and thus the hybrid label). To ensure the consistency of the formulation, duality is called upon to define the finite element variables that dissipate the same energy as the local fields which they model, the structural interpretation of the fundamental condition on the invariance of the inner product.

A second distinguishing feature of the approach followed here will also become apparent at this stage of the presentation, namely the discarding of the node concept and of the related frame functions. The node concept played a role so important in the development of conforming elements that it was also adapted and used in the development of hybrid elements. It is thought, however, that this concept constrains unnecessarily the development of the finite element method.

Important benefits can be gained by the alternative use of nodeless, naturally hierarchical approximation bases. It opens the choice of approximation functions, ranging from the application of digital and orthogonal functions, used in the hybrid–mixed formulation, to the rehabilitation of the use of the formal solutions of the governing wave equation, as exploited by the hybrid–Trefftz formulation. In addition, as these approximation bases are hierarchical, they lead naturally to adaptive procedures that can be fully exploited using high-order (super-) elements with an unconstrained geometry, as they do not need to be convex, simply connected or bounded.

### 2.3. Hybrid–mixed formulation

The hybrid–mixed formulation is derived by approximating simultaneously two fields in the domain of the element, namely the stresses and the displacements, and one field on its boundary, the displacements and the tractions (Cauchy stresses) in the stress and displacement models, respectively.

After stating the basic space approximation criteria, the finite element equations and the associated governing systems for the displacement and stress models of the hybrid–mixed formulation are presented and interpreted to clarify how the fundamental equations are being enforced.

In this formulation the approximation functions are not required to satisfy locally any of the fundamental field conditions. They are enforced on average and, consequently, neither the stress model nor the displacement model of the hybrid–mixed formulation will, in general, be able to generate statically or kinematically admissible solutions.

The strength of this formulation is, however, its ability to accommodate virtually any approximation basis, irrespective of the complexity of the problem under analysis. The flexibility in the selection of the approximation basis may also be important from a computational standpoint. For instance, the hybrid–mixed formulation can be implemented on Walsh and Wavelet approximation bases designed to exploit the digital architecture of the computer, see Freitas and Castro (1997).

The price paid by tailoring the approximation bases to the computer is the need to use a relatively high number of degrees of freedom to reach good levels of accuracy, as these functions are, in general, quite poor in information on the mechanics of the problem being modelled.

### 2.4. Hybrid formulation

The hybrid stress and displacement models are presented as the collapsed forms of the corresponding hybrid–mixed models for approximation bases that satisfy locally the equilibrium and compatibility conditions, respectively. It is then realised that only one field needs to be approximated in the domain of the elements, respectively, the stresses and the displacements in each model.

Besides involving less degrees of freedom for the same order in the approximation, when the relevant boundary and interelement conditions are conveniently enforced, the hybrid stress and displacement models generate solutions that are locally statically and kinematically admissible, respectively.

In fact, in the stress models, and irrespectively of the formulation, interelement continuity is enforced in terms of relative tractions, as in the displacement method of structural analysis. When this condition is strongly enforced, the solution is statically admissible because the direct stress

approximation in the hybrid formulation is constrained to satisfy locally the equilibrium condition in the domain of the element, see Almeida and Pereira (1996).

Conversely, in the displacement model, and again irrespectively of the formulation, interelement continuity is enforced in terms of relative displacements, as in the force method of structural analysis. When this condition is strongly enforced, the solution is kinematically admissible because in the hybrid formulation the strains are computed directly from the displacement approximation in the domain of the element, through the local compatibility conditions.

### 2.5. Hybrid–Trefftz formulation

In the next step of the presentation, the hybrid–Trefftz formulation is introduced as the strain of the hybrid formulation obtained by further constraining the domain approximation basis to satisfy all field equations, that is the governing wave equation in the present context. Therefore, the stress and displacement models of the hybrid–Trefftz formulation may also produce statically and kinematically admissible solutions, respectively. Exact solutions may thus be recovered whenever they can be encoded by suitable analytical expressions.

The major feature of the hybrid–Trefftz models is, however, the richness of information contained in the approximation bases in terms of the mechanics of the problem under analysis, meaning that they can generate highly accurate solutions using a relatively small number of degrees of freedom. Moreover, they combine the most interesting features of the conventional finite element and boundary element formulations, as they produce solving systems that are symmetric and sparse and described by structural arrays with boundary integral expressions.

At this stage of the presentation it will become apparent that the hybrid–Trefftz stress and displacement models relate directly with the HT-D and HT-T elements developed by Jirousek and his co-workers, see e.g. Jirousek and Wróblewski (1996).

The stress and displacement models of the hybrid–Trefftz formulation presented here extend into dynamics the quasi-static models originally presented as nodal and mesh boundary integral formulations in Freitas (1986). Due to the difficulties met in establishing a common comparison basis, only later were they identified with the hybrid–Trefftz approach and the stress and displacement models were subsequently labelled HTS and HTD, respectively.

This different labelling is retained to emphasise the direct relationship of the hybrid–Trefftz stress and displacement models with the corresponding models of the hybrid–mixed and hybrid formulations. In addition, and more importantly, the HT-D and HT-T designations are not adopted because they can be misleading. In fact, the HT-D and HT-T elements are stress and displacement elements, respectively, and not the inverse as it seems to be the generalised opinion.

This inaccuracy is probably caused by the identification of the HT-D and HT-T elements with the displacement and force methods of structural analysis, which is correct in terms of connectivity as it has been stated above for the hybrid formulation. However, what does distinguish stress from displacement elements is the field that is directly approximated in the domain of the element, and thus the confusion induced by the HT-D and HT-T labelling and derivation.

### 2.6. Theoretical framework

The general expressions obtained for the systems governing the response of a typical element are then assembled to build the solving system for the finite element mesh. The next step in the

approach adopted in the development of the alternative hybrid formulations and models consists in using mathematical programming equivalence and qualification conditions to establish the supporting theoretical framework.

It consists, in essence, in using basic results from mathematical programming equivalence theory to establish a posteriori the variational statements that can be associated with each finite element model derived directly from the fundamental conditions governing the problem being modelled. Other basic results in mathematical programming are also called upon to establish sufficient conditions for the existence, uniqueness and multiplicity of the finite element solution, the latter being useful to identify the causes of spurious modes in ill-designed hybrid elements.

This step in the derivation of hybrid elements is not illustrated in this paper. This matter is addressed in Freitas (1977a) and Freitas (1977b) in the context of the hybrid–Trefftz formulation, and the results presented there can be immediately extended to the hybrid and hybrid–mixed formulations.

### *2.7. Numerical implementation*

In the presentation followed here, after setting up the finite element solving systems the discussion proceeds immediately to the derivation of the solutions for both the free and forced vibration responses, which are combined using standard procedures to model the prescribed initial conditions.

The techniques used to set up, store and solve the resulting finite element systems of equations are commented only briefly because they are addressed in more detail in the references named at that stage of the presentation.

The paper closes with the presentation of illustrative numerical applications. The first set of tests is based on the analysis of the response of a simple rod to focus on the essential aspects that distinguish the relative performance of the alternative formulations and models. Two plate stretching applications are also presented to illustrate conveniently the implementation of the inter-element continuity conditions and the modelling of the displacement and stress fields.

## 3. Fundamental relations

Let $V$ represent the domain of the element and $\Gamma$ the enveloping surface, referred to Cartesian system $\mathbf{x}$, and $t$ define the time parameter. Assume that the variables describing the dynamic response of the element, say $\mathbf{v}$, are uncoupled in the forced and free vibration modes $\mathbf{v}_1$ and $\mathbf{v}_2$:

$$\mathbf{v}(\mathbf{x}, t) = \mathbf{v}_1(\mathbf{x}, t) + \mathbf{v}_2(\mathbf{x}, t) \quad \text{in } V \tag{1}$$

The amplitudes of the free vibration modes are so chosen as to satisfy the initial conditions of the problem, which are usually stated on the displacement and velocity fields:

$$\mathbf{u}_1(\mathbf{x}, 0) + \mathbf{u}_2(\mathbf{x}, 0) = \mathbf{u}_0(\mathbf{x}) \quad \text{in } V \tag{2}$$

$$\dot{\mathbf{u}}_1(\mathbf{x}, 0) + \dot{\mathbf{u}}_2(\mathbf{x}, 0) = \dot{\mathbf{u}}_0(\mathbf{x}) \quad \text{in } V \tag{3}$$

The fundamental relations governing linear elastostatic problems are stated as follows, where $j = 1$ and $j = 2$ denote the forced and free vibration modes, respectively:

$$\mathbf{D}\boldsymbol{\sigma}_j + \boldsymbol{\delta}_{j1}\mathbf{b} = \mathbf{d}\dot{\mathbf{u}}_j + \boldsymbol{\rho}\ddot{\mathbf{u}}_j \quad \text{in } V \tag{4}$$

$$\boldsymbol{\varepsilon}_j = \mathbf{D}^*\mathbf{u}_j \quad \text{in } V \tag{5}$$

$$\boldsymbol{\sigma}_j = \mathbf{k}\boldsymbol{\varepsilon}_j + \mathbf{c}\dot{\boldsymbol{\varepsilon}}_j + \boldsymbol{\delta}_{j1}(\boldsymbol{\sigma}_\theta - \mathbf{k}\boldsymbol{\varepsilon}_\theta) \quad \text{in } V \tag{6}$$

$$\mathbf{N}\boldsymbol{\sigma}_j = \boldsymbol{\delta}_{j1}\mathbf{t}_\Gamma \quad \text{on } \Gamma_\sigma \tag{7}$$

$$\mathbf{u}_j = \boldsymbol{\delta}_{j1}\mathbf{u}_\Gamma \quad \text{on } \Gamma_u \tag{8}$$

In the conditions of dynamic equilibrium and compatibility (4) and (5), vectors $\boldsymbol{\sigma}_j$ and $\boldsymbol{\varepsilon}_j$ collect the independent components of the stress and strain tensors, respectively, $\mathbf{b}$ is the body force vector, matrices $\mathbf{d}$ and $\boldsymbol{\rho}$ collect, respectively, the relevant structural damping and specific mass coefficients and $\delta_{jk}$ denotes the Kronecker symbol ($j = 1, 2; k = 1$). As a geometrically linear model is assumed, the differential equilibrium and compatibility operators $\mathbf{D}$ and $\mathbf{D}^*$ are linear and adjoint.

In the linear description (6) for the elasticity condition, $\mathbf{k}$ and $\mathbf{c}$ are the stiffness and material damping matrices and vectors $\boldsymbol{\sigma}_\theta$ and $\boldsymbol{\varepsilon}_\theta$ are used to represent either residual stresses or strains.

Equations (7) and (8) define the static and kinematic boundary conditions, respectively. Vectors $\mathbf{t}_\Gamma$ and $\mathbf{u}_\Gamma$ identify the tractions (Cauchy stresses) and the displacements prescribed on the complementary portions $\Gamma_\sigma$ and $\Gamma_u$ of the boundary. Mixed boundary conditions are assumed to be accounted for in the usual notation for geometric complementarity: $\Gamma = \Gamma_\sigma \bigcup \Gamma_\mathbf{u}$; $\varnothing = \Gamma_\sigma \bigcap \Gamma_\mathbf{u}$. In eqn (7), the boundary equilibrium matrix $\mathbf{N}$ collects the components of the unit outward normal vector associated with the differential operators present in the domain equilibrium matrix $\mathbf{D}$.

The equations above hold for inhomogeneous and multiphase media. For instance, for the two-phase problem of wave propagation in saturated poroelastic media, vector $\boldsymbol{\sigma}\{\boldsymbol{\varepsilon}\}$ combines the stress $\{$strain$\}$ components in the solid phase with the pore fluid stress $\{$fluid content$\}$ and vector $\mathbf{u}\{\mathbf{b}\}$ lists the displacement components of the solid phase and the seepage displacement parameter $\{$equivalent body forces of the solid and fluid phases$\}$. All the remaining arrays in system (4)–(8) are organised accordingly.

## 4. Time discretization

Let the generic variable (1) be expanded in the time series (9) in the interval $0 \leqslant t \leqslant T$ and use the dual transformation (10) to define the corresponding Fourier coefficients:

$$\mathbf{v}_j(\mathbf{x}, t) = \sum_{n=-\infty}^{+\infty} \mathbf{v}_{jn}(\mathbf{x})\, \mathrm{e}^{i\omega_{jn}} \tag{9}$$

$$\mathbf{v}_{jn} = \frac{1}{T}\int_0^T \mathbf{v}_j\, \mathrm{e}^{-i\omega_{jn}t}\, \mathrm{d}t \tag{10}$$

The following sequence of uncoupled, time independent problems is obtained using the time approximation basis to enforce on average each of the fundamental equations in system (4)–(8):

$$\mathbf{D}\boldsymbol{\sigma}_{jn} + \boldsymbol{\rho}_{jn}\omega_{jn}^2\mathbf{u}_{jn} + \boldsymbol{\delta}_{j1}\mathbf{b}_n = \mathbf{0} \quad \text{in } V \tag{11}$$

$$\boldsymbol{\varepsilon}_{jn} = \mathbf{D}^{*}\mathbf{u}_{jn} \quad \text{in } V \tag{12}$$

$$\boldsymbol{\sigma}_{jn} = \mathbf{k}_{jn}\boldsymbol{\varepsilon}_{jn} + \boldsymbol{\delta}_{j1}\boldsymbol{\sigma}_{rn} \quad \text{in } V \tag{13}$$

$$\mathbf{N}\boldsymbol{\sigma}_{jn} = \boldsymbol{\delta}_{j1}\mathbf{t}_{\Gamma n} \quad \text{on } \Gamma_{\boldsymbol{\sigma}} \tag{14}$$

$$\mathbf{u}_{jn} = \boldsymbol{\delta}_{j1}\mathbf{u}_{\Gamma n} \quad \text{on } \Gamma_{\mathbf{u}} \tag{15}$$

As it is detailed in Appendix A, to avoid the implementation of approximation (9) on the velocity and acceleration fields, the average enforcement of the equilibrium and elasticity eqns (4) and (6) is integrated by parts and the response of the structure is assumed to be periodic in the actual or fictitious time interval $T$. The amplitudes of the free and forced vibration modes are, however, determined from the following description for the initial conditions (2) and (3):

$$\sum_{n=-\infty}^{+\infty} (\mathbf{u}_{1n} + \mathbf{u}_{2n}) = \mathbf{u}_0 \quad \text{in } V \tag{16}$$

$$i \sum_{n=-\infty}^{+\infty} (\boldsymbol{\omega}_{1n}\mathbf{u}_{1n} + \boldsymbol{\omega}_{2n}\mathbf{u}_{2n}) = \dot{\mathbf{u}}_0 \quad \text{in } V \tag{17}$$

In the equations above, the following notation is used for the generalised mass and stiffness matrices and for the generalised residual stress vector:

$$\boldsymbol{\rho}_{jn} = \boldsymbol{\rho} - i\boldsymbol{\omega}_{jn}^{-1}\mathbf{d}$$

$$\mathbf{k}_{jn} = \mathbf{k} + i\boldsymbol{\omega}_{jn}\mathbf{c}$$

$$\boldsymbol{\sigma}_{rn} = \boldsymbol{\sigma}_{\theta n} - \mathbf{k}\boldsymbol{\varepsilon}_{\theta n}$$

For later use, the elasticity relation (14) is also written in the alternative flexibility format:

$$\boldsymbol{\varepsilon}_{jn} = \mathbf{f}_{jn}\boldsymbol{\sigma}_{jn} + \boldsymbol{\delta}_{j1}\boldsymbol{\varepsilon}_{rn}$$

$$\mathbf{f}_{jn} = \mathbf{k}_{jn}^{-1}$$

$$\boldsymbol{\varepsilon}_{rn} = -\mathbf{f}_{jn}\boldsymbol{\sigma}_{rn} \tag{18}$$

For simplicity of the presentation, subscript $j$, identifying the forced ($j = 1$) and free ($j = 2$) vibration modes, is now dropped from the notation. The particular terms $\delta_{jk}\mathbf{v}_n$ are written simply as $\mathbf{v}_n$.

## 5. Hybrid–mixed formulation

In the most general formulation set, the hybrid–mixed formulation, the space discretization develops from the independent approximation of the stress and displacement fields in the domain of the finite element, as stated by eqns (19) and (20), where matrices, $\mathbf{S}_{Vn}$ and $\mathbf{U}_{Vn}$ collect appropriate approximation functions and vectors $\mathbf{X}_{Vn}$ and $\mathbf{q}_{Vn}$ list the associated weights:

$$\boldsymbol{\sigma}_n = \mathbf{S}_{Vn}\mathbf{X}_{Vn} + \boldsymbol{\sigma}_{pn} \quad \text{in } V \tag{19}$$

$$\mathbf{u}_n = \mathbf{U}_{Vn}\mathbf{q}_{Vn} + \mathbf{u}_{pn} \quad \text{in } V \tag{20}$$

In these approximations, vectors $\boldsymbol{\sigma}_{pn}$ and $\mathbf{u}_{pn}$ are used to model particular solutions, for instance those associated with body forces, specific boundary conditions or residual stresses and strains.

As the node concept is not used, the bases $\mathbf{S}_{Vn}$ and $\mathbf{U}_{Vn}$ can be built on hierarchical sets of approximation functions, at the minor cost of losing an explicit physical interpretation for the weighing vectors $\mathbf{X}_{Vn}$ and $\mathbf{q}_{Vn}$, which represent generalised stresses and displacements.

The approximation functions may include the terms necessary to model relevant local effects, namely the fundamental solutions associated with cracks. However, and in principle, they are not required to satisfy the field or boundary conditions of the problem under analysis.

The dual transformations (21) and (22) of definitions (19) and (20) define the generalised strain vector, $\mathbf{e}_n$, and the generalised body force vector, $\mathbf{Q}_{bn}$, that dissipate on their dual generalised stresses and displacements the same energy as the continuum fields they are associated with:

$$\mathbf{e}_n = \int \mathbf{S}_{Vn}^t \boldsymbol{\varepsilon}_n \, \mathrm{d}V \tag{21}$$

$$\mathbf{Q}_{bn} = \int \mathbf{U}_{Vn}^t \mathbf{b}_n \, \mathrm{d}V$$

$$\mathbf{X}_{Vn}^t \mathbf{e}_n = \int (\boldsymbol{\sigma}_n - \boldsymbol{\sigma}_{pn})^t \boldsymbol{\varepsilon}_n \, \mathrm{d}V$$

$$\mathbf{q}_{Vn}^t \mathbf{Q}_{bn} = \int (\mathbf{u}_n - \mathbf{u}_{pn})^t \mathbf{b}_n \, \mathrm{d}V \tag{22}$$

The definitions above for the (prescribed) generalised body forces and for the (free) generalised strains are used to enforce consistently (on average, in the Galerkin-weighed residual form) the equilibrium and the compatibility conditions (11) and (12), respectively:

$$\int \mathbf{U}_{Vn}^t (\mathbf{D}\boldsymbol{\sigma}_n + \boldsymbol{\rho}_n \omega_n^2 \mathbf{u}_n + \mathbf{b}_n) \, \mathrm{d}V = \mathbf{0} \tag{23}$$

$$\int \mathbf{S}_{Vn}^t \boldsymbol{\varepsilon}_n \, \mathrm{d}V = \int \mathbf{S}_{Vn}^t \mathbf{D}^* \mathbf{u}_n \, \mathrm{d}V \tag{24}$$

It is stressed that, when a complex basis is used to set up the approximation matrix and define its weighing vector, say $\mathbf{A}$ and $\mathbf{w}$, in the notation followed here $\mathbf{A}^t$ and $\mathbf{w}^t$ denote the transpose of their conjugates.

The two alternative displacement and stress models of the hybrid–mixed formulation are obtained depending on whether interelement continuity is enforced on the boundary tractions or on the boundary displacements.

At finite element level, different definitions hold for the static and kinematic boundaries, $\Gamma_\sigma$ and $\Gamma_u$, for the alternative stress and displacement models. In the stress {displacement} model, the static {kinematic} boundary is defined as the portion of the envelope whereon the displacements {tractions} are not known a priori. The complementary portion of the envelope defines the kinematic {static} boundary of the stress {displacement} element.

The displacement model is designed to enforce explicitly the boundary displacement continuity condition. To this effect, the boundary tractions are also approximated directly in form (25) and the dual transformation (26) for the generalised boundary displacements, $\mathbf{v}_{\Gamma n}$, is used to enforce on average the kinematic boundary condition (15) for the assumed displacements (20):

$$\mathbf{t}_n = \mathbf{S}_{\Gamma n}\mathbf{X}_{\Gamma n} \quad \text{on } \Gamma_{\mathbf{u}} \tag{25}$$

$$\mathbf{v}_{\Gamma n} = \int \mathbf{S}_{\Gamma n}^t \mathbf{u}_{\Gamma n}\, \mathrm{d}\Gamma_{\mathbf{u}} \tag{26}$$

$$\int \mathbf{S}_{\Gamma n}^t \mathbf{u}_n\, \mathrm{d}\Gamma_{\mathbf{u}} = \int \mathbf{S}_{\Gamma n}^t \mathbf{u}_{\Gamma n}\, \mathrm{d}\Gamma_{\mathbf{u}} \tag{27}$$

Complementarily, in the stress model it is the boundary displacements which are also approximated directly, as stated by eqns (28), and the dual generalised tractions, $\mathbf{Q}_{\Gamma n}$, are used to enforce the static boundary condition (14) for the assumed stresses (19):

$$\mathbf{u}_n = \mathbf{U}_{\Gamma n}\mathbf{q}_{\Gamma n} \quad \text{on } \Gamma_{\boldsymbol{\sigma}} \tag{28}$$

$$\mathbf{Q}_{\Gamma n} = \int \mathbf{U}_{\Gamma n}^t \mathbf{t}_{\Gamma n}\, \mathrm{d}\Gamma_{\boldsymbol{\sigma}} \tag{29}$$

$$\int \mathbf{U}_{\Gamma n}^t \mathbf{N}\boldsymbol{\sigma}_n\, \mathrm{d}\Gamma_{\boldsymbol{\sigma}} = \int \mathbf{U}_{\Gamma n}^t \mathbf{t}_{\Gamma n}\, \mathrm{d}\Gamma_{\boldsymbol{\sigma}} \tag{30}$$

As for the domain approximation, the alternative boundary bases $\mathbf{S}_{\Gamma n}$ and $\mathbf{U}_{\Gamma n}$ are hierarchical and are not required to satisfy any continuity condition a priori. The associated weights $\mathbf{X}_{\Gamma n}$ and $\mathbf{q}_{\Gamma n}$ represent generalised tractions and displacements, respectively. As for the domain approximations, definitions (26) and (29) ensure the necessary energy balance on the related boundary fields:

$$\mathbf{X}_{\Gamma n}^t \mathbf{v}_{\Gamma n} = \int \mathbf{t}_n^t \mathbf{u}_{\Gamma n}\, \mathrm{d}\Gamma_{\mathbf{u}}$$

$$\mathbf{q}_{\Gamma n}^t \mathbf{Q}_{\Gamma n} = \int \mathbf{u}_n^t \mathbf{t}_{\Gamma n}\, \mathrm{d}\Gamma_{\boldsymbol{\sigma}}$$

The main characteristics of the stress and displacement models of the hybrid–mixed formulation are summarised in Tables 1–3 to support the derivation of the finite element equations resulting

Table 1
Hybrid–mixed finite element approximations

| Type of model | Approximations | |
|---|---|---|
| | In the domain | On the boundary |
| Stress | Stresses and | Displacements |
| Displacement | displacements | Tractions |

Table 2
Hybrid–mixed enforcement of the field conditions

| Type of model | Field conditions | |
|---|---|---|
| | Locally satisfied | Explicitly enforced |
| Stress and displacement | None | All |

Table 3
Enforcement of the boundary conditions

| Type of model | Natural boundary conditions | | Interelement boundary conditions | |
|---|---|---|---|---|
| | Locally satisfied | Explicitly enforced | Locally satisfied | Explicitly enforced |
| Stress | Kinematic | Static | None | Static |
| Displacement | Static | Kinematic | None | Kinematic |

from the fundamental space approximations stated above. This derivation is so performed as to obtain equilibrium and compatibility equations that are independent of the constitutive relations and elasticity equations independent of the static and kinematic admissibility conditions.

Hence, the finite element descriptions of statics and kinematics given here hold for any geometrically linear problem and the finite element description of elasticity can be used in modelling physically linear problems. To generalise the finite element model to geometrically {physically} non-linear problems it suffices to extend the finite element description of statics and kinematics {elasticity} while preserving the finite element description of elasticity {statics and kinematics}.

## 6. Hybrid–mixed displacement model

Equations (31) and (32) define the description of kinematics for the hybrid–mixed displacement model. They are obtained by inserting the displacement approximation (20) in the average enforcement of the compatibility and displacement continuity conditions, stated by eqns (24) and (27), respectively, together with definitions (21) and (26):

$$\mathbf{e} = \mathbf{B}_V^t \mathbf{q}_V + \mathbf{e}_p \tag{31}$$

$$\mathbf{v}_\Gamma = \mathbf{B}_\Gamma^t \mathbf{q}_V + \mathbf{v}_p \tag{32}$$

To simplify the presentation, the definitions of the arrays present in the equations derived for the displacement and stress models are removed from the main text and collected in Appendix B. Moreover, subscript $n$ identifying the $n$-th (free or forced) frequency $\omega_{jn}$ mode is dropped in all equations from this point onwards.

In an unassembled element, the displacements vector, $\mathbf{u}_\Gamma$, plays a dual role. It can be used either to represent the displacements prescribed on the boundary of the finite elements sharing the kinematic boundary of the structure or the unknown displacements on the boundary of an adjacent element. This latter indeterminacy is solved when the finite element mesh is assembled, by enforcing interelement continuity on the generalised discontinuities $\mathbf{v}_\Gamma$. Vectors $\mathbf{e}_p$ and $\mathbf{v}_p$ are prescribed, as they represent the contributions to the generalised strains and discontinuities of the particular solution $\mathbf{u}_p$ in the displacement approximation (20).

To obtain the description of statics in the dual form of eqns (31) and (32), the average enforcement (23) of the local equilibrium conditions is first integrated by parts:

$$-\int (\mathbf{D}^*\mathbf{U}_V)^t\boldsymbol{\sigma}\,\mathrm{d}V+\int \mathbf{U}_V^t\mathbf{N}\boldsymbol{\sigma}\,\mathrm{d}\Gamma+\omega^2\int \mathbf{U}_V^t\boldsymbol{\rho}\mathbf{u}\,\mathrm{d}V+\int \mathbf{U}_V^t\mathbf{b}\,\mathrm{d}V=\mathbf{0} \tag{33}$$

The emerging boundary term is uncoupled to enforce directly the static boundary condition (14) together with the approximations for the stresses, displacements and tractions, as stated by equations (19), (20) and (25), respectively, to yield the following expression,

$$\mathbf{B}_V\mathbf{X}_V-\mathbf{B}_\Gamma\mathbf{X}_\Gamma-\omega^2\mathbf{M}_V\mathbf{q}_V=\mathbf{Q}_b+\mathbf{Q}_t-\mathbf{Q}_p-\mathbf{Q}_f \tag{34}$$

where $\mathbf{M}_V$ is the mass matrix and $\mathbf{Q}_p$, $\mathbf{Q}_f$ and $\mathbf{Q}_t$ are vectors associated with the particular solution terms in the stress and displacement approximations and with the tractions prescribed on the boundary of the unassembled element (see Appendix B).

The resulting eqn (34) represents the finite element (weak) static admissibility condition, as it combines the equilibrium and static boundary conditions which, in general, will not be satisfied locally. Similarly, the solutions obtained through eqns (31) and (32) are kinematically admissible only in the weak sense.

To obtain the following description for elasticity, it suffices to insert the constitutive relations in the flexibility format (18) and the stress approximation (19) in definition (21) for the generalised strains:

$$\mathbf{e}=\mathbf{F}_V\mathbf{X}_V+\mathbf{e}_0 \tag{35}$$

$\mathbf{F}_V$ denotes the flexibility matrix of the element and the prescribed generalised strain vector $\mathbf{e}_0$ combines the contributions of the residual strains and of the particular stress solution.

The elementary governing system (36) given in Table 4 is obtained combining the descriptions found for statics, kinematics and elasticity. The definitions for the stipulation force and dis-

Table 4
Hybrid–mixed governing systems (refer to Appendix B)

| Displacement model (36) | Stress model (37) |
|---|---|
| $\begin{bmatrix} -\omega^2\mathbf{M}_V & \mathbf{B}_V & -\mathbf{B}_\Gamma \\ \mathbf{B}_V^t & -\mathbf{F}_V & \mathbf{O} \\ -\mathbf{B}_\Gamma^t & \mathbf{O} & \mathbf{O} \end{bmatrix}\begin{Bmatrix} \mathbf{q}_V \\ \mathbf{X}_V \\ \mathbf{X}_\Gamma \end{Bmatrix}=\begin{Bmatrix} \mathbf{f}_V \\ \mathbf{d}_V \\ \mathbf{d}_\Gamma \end{Bmatrix}$ | $\begin{bmatrix} \mathbf{F}_V & \mathbf{A}_V & -\mathbf{A}_\Gamma \\ \mathbf{A}_V^t & \omega^2\mathbf{M}_V & \mathbf{O} \\ -\mathbf{A}_\Gamma^t & \mathbf{O} & \mathbf{O} \end{bmatrix}\begin{Bmatrix} \mathbf{X}_V \\ \mathbf{q}_V \\ \mathbf{q}_\Gamma \end{Bmatrix}=\begin{Bmatrix} \mathbf{d}_V \\ \mathbf{f}_V \\ \mathbf{f}_\Gamma \end{Bmatrix}$ |

placement vectors $\mathbf{f}_V$, $\mathbf{d}_V$ and $\mathbf{d}_\Gamma$, are given in Appendix B. In the notation used in Table 4, subscripts $V$ and $\Gamma$ identify the finite element arrays defined by domain and boundary integral expressions, respectively.

## 7. Hybrid–mixed stress model

The elementary governing system (37) for the hybrid–mixed stress model is obtained by combination of the following description for statics and kinematics with eqn (35) for elasticity:

$$\mathbf{A}_V^t\mathbf{X}_V+\omega^2\mathbf{M}_V\mathbf{q}_V+\mathbf{Q}_b+\mathbf{Q}_p+\mathbf{Q}_f=\mathbf{0} \tag{38}$$

$$\mathbf{A}_\Gamma^t\mathbf{X}_V=\mathbf{Q}_\Gamma-\mathbf{Q}_t \tag{39}$$

$$\mathbf{e}=-\mathbf{A}_V\mathbf{q}_V+\mathbf{A}_\Gamma\mathbf{q}_\Gamma+\mathbf{e}_\Gamma-\mathbf{e}_p \tag{40}$$

Equations (38) and (39) for statics are obtained from the average enforcement of the field and boundary equilibrium conditions (23) and (30), respectively, for the assumed stress and displacement approximations (19) and (20).

To obtain the dual description (40) of kinematics, the average enforcement of the field compatibility condition (24) is first integrated by parts:

$$\int\mathbf{S}_V^t\boldsymbol{\varepsilon}\,\mathrm{d}V=-\int(\mathbf{D}\mathbf{S}_V)^t\mathbf{u}\,\mathrm{d}V+\int(\mathbf{N}\mathbf{S}_V)^t\mathbf{u}\,\mathrm{d}\Gamma \tag{41}$$

In the resulting definition for the generalised strains (21), the boundary term is uncoupled to enforce separately the kinematic boundary condition (15) and the approximation for the displacements, both in the domain and on the boundary, as stated by eqns (20) and (28).

## 8. Hybrid formulation

The stress and displacement models of the hybrid formulation are obtained from the corresponding models of the hybrid–mixed formulation by requiring the domain approximation functions to satisfy locally the equilibrium and the compatibility field conditions, respectively. As it is stated in Tables 5 and 6, it is then found that only one field has to be approximated in the finite element domain.

Table 5
Hybrid finite element approximations

| Type of model | Approximations | |
|---|---|---|
| | In the domain | On the boundary |
| Stress | Stresses | Displacements |
| Displacement | Displacements | Tractions |

Table 6
Hybrid enforcement of the field conditions

| Type of model | Field conditions | |
|---|---|---|
| | Locally satisfied | Explicitly enforced |
| Stress | Equilibrium | Compatibility and elasticity |
| Displacement | Compatibility | Equilibrium and elasticity |

Table 7
Hybrid governing systems (refer to Appendix B)

| Displacement model (42) | Stress model (43) |
|---|---|
| $\begin{bmatrix} \mathbf{K}_V - \omega^2 \mathbf{M}_V & -\mathbf{B}_\Gamma \\ -\mathbf{B}_\Gamma^t & \mathbf{O} \end{bmatrix} \begin{Bmatrix} \mathbf{q}_V \\ \mathbf{X}_\Gamma \end{Bmatrix} = \begin{Bmatrix} \mathbf{f}_V \\ \mathbf{d}_\Gamma \end{Bmatrix}$ | $\begin{bmatrix} \mathbf{F}_V - \omega^{-2} \tilde{\mathbf{M}}_V & -\mathbf{A}_\Gamma \\ -\mathbf{A}_\Gamma^t & \mathbf{O} \end{bmatrix} \begin{Bmatrix} \mathbf{X}_V \\ \mathbf{q}_\Gamma \end{Bmatrix} = \begin{Bmatrix} \mathbf{d}_V \\ \mathbf{f}_\Gamma \end{Bmatrix}$ |

In the hybrid stress {displacement} model, except for the equilibrium condition (11) {compatibility condition (12)}, all the remaining field and boundary conditions are still enforced in a weighed residual form. A strong enforcement of the interelement and natural static boundary condition (14) {kinematic boundary condition (15)} is now sufficient to ensure static {kinematic} admissibility.

As it is shown below, the resulting governing systems, presented in Table 7, embody the same properties of the systems of their hybrid–mixed parents but involve fewer degrees of freedom, as only one field needs to be approximated in the domain of the finite element. In addition, the hybrid finite element equilibrium and compatibility matrices have boundary integral expressions.

## 9. Hybrid displacement model

Within the framework of the hybrid–mixed displacement model, assume further that the displacement approximation (20) is used to determine a compatible strain field, so that the average enforcement (24) of the compatibility condition (12) is rendered trivial:

$$\boldsymbol{\varepsilon} = \mathbf{E}_V \mathbf{q}_V + \boldsymbol{\varepsilon}_p \quad \text{in } V \tag{44}$$

$$\mathbf{E}_V = \mathbf{D}^* \mathbf{U}_V \tag{45}$$

$$\boldsymbol{\varepsilon}_p = \mathbf{D}^* \mathbf{u}_p \tag{46}$$

The description for kinematics reduces now to the weighed enforcement of the kinematic

boundary condition (15), as stated by eqn (32). Definition (44) implies the existence of a dual generalised stress field, $\mathbf{X}$, to ensure consistency in energy dissipation in the finite element model:

$$\mathbf{X} = \int \mathbf{E}_V^t \boldsymbol{\sigma} \, \mathrm{d}V$$

$$\mathbf{q}_V^t \mathbf{X} = \int (\boldsymbol{\varepsilon} - \boldsymbol{\varepsilon}_p)^t \boldsymbol{\sigma} \, \mathrm{d}V \tag{47}$$

The explicit approximation (19) of the stress field is abandoned as a consequence of introducing the generalised stresses (47) as a free term in the average equilibrium condition (23):

$$\mathbf{X} = \mathbf{B}_\Gamma \mathbf{X}_\Gamma + \omega^2 \mathbf{M}_V \mathbf{q}_V + \mathbf{Q}_t + \mathbf{Q}_b + \mathbf{Q}_f \tag{48}$$

The equation above is the new description for Statics, with all the remaining terms being defined as for the hybrid–mixed displacement model, as the boundary traction approximation (25) is still assumed.

Definitions (44) and (47) for the assumed strains and for the generalised stresses are used to enforce the elasticity relations in the stiffness format (13), to yield the following expression,

$$\mathbf{X} = \mathbf{K}_V \mathbf{q}_V + \mathbf{X}_0 \tag{49}$$

where $\mathbf{K}_V$ is the finite element stiffness matrix and $\mathbf{X}_0$ is the prescribed stress vector consistent with the effects associated with the residual stresses and with the strains induced by the particular solution in the displacement approximation (see Appendix B).

The governing system (42) is obtained by combining eqns (32), (48) and (49) for kinematics, statics and elasticity, respectively. System (42) is, in essence, a particular version of system (36) derived for the hybrid–mixed displacement model, where now the finite element compatibility condition (31) is locally satisfied. It does not correspond to the condensation of system (36) in the generalised displacements and tractions $\mathbf{q}_V$ and $\mathbf{X}_\Gamma$.

## 10. Hybrid stress model

Assume that the stress approximation (19) is constrained to satisfy locally the equilibrium condition (11) by selecting the following definition for the displacement field instead of approximation (20):

$$\mathbf{u} = \mathbf{U}_V \mathbf{X}_V + \mathbf{u}_p \quad \text{in } V \tag{50}$$

$$\mathbf{D}\mathbf{S}_V = -\omega^2 \boldsymbol{\rho} \mathbf{U}_V \tag{51}$$

$$\mathbf{D}\boldsymbol{\sigma}_p = -\omega^2 \boldsymbol{\rho} \mathbf{u}_p - \mathbf{b} \tag{52}$$

Enforcement (23) of the equilibrium condition is identically satisfied and the finite element description for statics in the hybrid stress model reduces to the weighed enforcement (39) of the static boundary condition used in the stress model of the hybrid–mixed formulation.

Assumptions (50)–(52) are inserted in the weighed enforcement (41) of the field compatibility

condition (12) to yield, together with definition (21), the following description for kinematics, where $\tilde{\mathbf{M}}_V$ is the mobility matrix and vector $\mathbf{e}_u$ collects the generalised strains consistent with the body forces and the particular solution in the stress approximation (see Appendix B):

$$\mathbf{e} = \omega^{-2}\tilde{\mathbf{M}}_V\mathbf{X}_V + \mathbf{A}_\Gamma\mathbf{q}_\Gamma + \mathbf{e}_\Gamma - \mathbf{e}_u \tag{53}$$

The elementary governing system (43) is obtained by combining the elasticity relation (35) with eqns (39) and (53) for statics and kinematics, respectively. System (43) does not correspond to the condensation of system (37) in the generalised stresses $\mathbf{X}_V$ and boundary displacements $\mathbf{q}_\Gamma$, but replaces the system found for the hybrid–mixed stress model under the constraint of satisfying locally the domain equilibrium condition (11).

## 11. Hybrid–Trefftz formulation

The hybrid–Trefftz stress and displacement models are derived from the corresponding hybrid models by further constraining the field approximation functions to satisfy locally the governing wave equation, as stated in Table 8. The information contained in Tables 3 and 5 still holds for the hybrid–Trefftz formulation and models.

The displacement approximation functions are now selected from the solution set of the Helmholtz eqn (54), obtained by combining the fundamental conditions (11)–(13), yielding the sufficient conditions (55) and (56) on the displacement approximation (20):

$$(\mathbf{DkD}^* + \omega^2\boldsymbol{\rho})\mathbf{u} + \mathbf{D}\boldsymbol{\sigma}_r + \mathbf{b} = \mathbf{0} \quad \text{in } V \tag{54}$$

$$(\mathbf{DkD}^* + \omega^2\boldsymbol{\rho})\mathbf{U}_V = \mathbf{O} \quad \text{in } V \tag{55}$$

$$(\mathbf{DkD}^* + \omega^2\boldsymbol{\rho})\mathbf{u}_p + \mathbf{D}\boldsymbol{\sigma}_r + \mathbf{b} = \mathbf{0} \quad \text{in } V \tag{56}$$

Consequently, the corresponding strain fields defined by eqns (45) and (46) are now assumed to be associated with the elastic stresses that satisfy the equilibrium conditions (51) and (52):

$$\mathbf{S}_V = \mathbf{kE}_V \tag{57}$$

$$\boldsymbol{\sigma}_p = \mathbf{k}\boldsymbol{\varepsilon}_p + \boldsymbol{\sigma}_r \tag{58}$$

Table 8
Hybrid–Trefftz enforcement of the field conditions

| Type of model | Field conditions | |
|---|---|---|
| | Locally satisfied | Explicitly enforced |
| Stress | All | Compatibility and elasticity |
| Displacement | | Equilibrium and elasticity |

Table 9
Hybrid–Trefftz governing systems (refer to Appendix B)

| Displacement model (59) | Stress model (60) |
|---|---|
| $\begin{bmatrix} \mathbf{D}_\Gamma & -\mathbf{B}_\Gamma \\ -\mathbf{B}_\Gamma^t & \mathbf{O} \end{bmatrix} \begin{Bmatrix} \mathbf{q}_V \\ \mathbf{X}_\Gamma \end{Bmatrix} = \begin{Bmatrix} \mathbf{f}_V \\ \mathbf{d}_\Gamma \end{Bmatrix}$ | $\begin{bmatrix} \mathbf{D}_\Gamma & -\mathbf{A}_\Gamma \\ -\mathbf{A}_\Gamma^t & \mathbf{O} \end{bmatrix} \begin{Bmatrix} \mathbf{X}_V \\ \mathbf{q}_\Gamma \end{Bmatrix} = \begin{Bmatrix} \mathbf{d}_\Gamma \\ \mathbf{f}_\Gamma \end{Bmatrix}$ |

As it is shown in Table 9, the finite element governing systems for the two alternative hybrid–Trefftz models are structurally identical to those derived for the corresponding hybrid models. However, and consequent upon the Trefftz constraints (55) and (56), it is now found that all the intervening finite element arrays are defined by boundary integral expressions, thus reducing in one order the dimension of the problem under analysis. Moreover, the computation of the mass and elasticity matrices is replaced by the determination of the equivalent elastodynamic matrix, $\mathbf{D}_\Gamma$.

## 12. Hybrid–Trefftz models

Let constraint (45) be enforced in definition (B6), given in Appendix B, for the finite element stiffness matrix. After integrating by parts of resulting equation, the following results are found enforcing conditions (51) and (57) and recalling definition (B2) for the mass matrix:

$$\mathbf{K}_V = -\int \mathbf{U}_V^t \mathbf{D}\mathbf{k}\mathbf{E}_V \, \mathrm{d}V + \int \mathbf{U}_V^t \mathbf{N}\mathbf{k}\mathbf{E}_V \, \mathrm{d}\Gamma$$

$$\mathbf{K}_V = \omega^2 \mathbf{M}_V + \mathbf{D}_\Gamma \tag{61}$$

$$\mathbf{D}_\Gamma = \int \mathbf{U}_V^t \mathbf{N}\mathbf{S}_V \, \mathrm{d}\Gamma \tag{62}$$

Using results (22), (45), (52), (58) and (B4), and processing in a similar way definition (B7) for the generalised residual stresses, the following alternative description is obtained:

$$\mathbf{X}_0 = \mathbf{Q}_b + \mathbf{Q}_f + \mathbf{X}_{0\Gamma}$$

$$\mathbf{X}_{0\Gamma} = \int \mathbf{U}_V^t \mathbf{N}\boldsymbol{\sigma}_p \, \mathrm{d}\Gamma \tag{63}$$

The finite element governing system (59) from the hybrid–Trefftz displacement model is obtained by enforcing results (61) and (62) in the hybrid displacement model system (42). Definition (B5) for array $\mathbf{d}_\Gamma$ still holds and expression (B8) is replaced by the following boundary integral result:

$$\mathbf{f}_\Gamma = \mathbf{Q}_t - \mathbf{X}_{0\Gamma}$$

To obtain the hybrid–Trefftz stress model, conditions (45) and (57) are inserted in definition (B1) for the flexibility matrix, the resulting expression is integrated by parts to enforce the local equilibrium condition (51). Recalling results (62) and (B10), the following alternative description is thus found:

$$\mathbf{F}_V = \boldsymbol{\omega}^{-2}\tilde{\mathbf{M}}_V + \mathbf{D}_\Gamma \tag{64}$$

The equivalent result for the residual strains is obtained treating similarly definition (B11):

$$\begin{aligned} \mathbf{e}_0 &= \mathbf{e}_{0\Gamma} - \mathbf{e}_u \\ \mathbf{e}_{0\Gamma} &= \int (\mathbf{N}\mathbf{S}_V)^t \mathbf{u}_p \, \mathrm{d}\Gamma \end{aligned} \tag{65}$$

The finite element governing system (60) for the hybrid–Trefftz stress model is derived by enforcing results (64) and (65) in the hybrid stress model system (43). Definition (B9) still holds in the stipulation vector, while definition (B12) is replaced by the following boundary integral expression:

$$\mathbf{d}_\Gamma = \mathbf{e}_\Gamma - \mathbf{e}_{0\Gamma}$$

## 13. Static phase in the response

The static phase in the dynamic response of the structure is modelled by the zero-th order solution of the governing system (11)–(15). The expressions presented in Tables 4, 7, and 9 for the finite element solving system, in the alternative hybrid–mixed, hybrid and hybrid–Trefftz formats are still valid, provided that they are conveniently specialised by letting $\boldsymbol{\omega}_0 = 0$.

Because they are not subjected to particular constraints, the approximation functions adopted in the $n$-th order dynamic solutions can also be used to solve the static phase in the hybrid–mixed models and in the hybrid displacement model.

In the hybrid stress model, assumption (50) on the displacement field is removed. Instead of conditions (51) and (52), to satisfy the local equilibrium condition (11) it suffices now to require the stress approximation functions to represent self-equilibrated fields and to select a particular stress approximation that equilibrates the body forces:

$$\begin{aligned} \mathbf{D}\mathbf{S}_V &= \mathbf{O} \\ \mathbf{D}\boldsymbol{\sigma}_p + \mathbf{b} &= \mathbf{0} \end{aligned} \tag{66}$$

In the hybrid–Trefftz displacement model, the zero-th order displacement approximation functions are the solutions of the Navier equation that replaces the Helmholtz eqn (54), and the Trefftz constraints (55) and (56) are replaced by the following:

$$\begin{aligned} \mathbf{D}\mathbf{k}\mathbf{D}^*\mathbf{U}_V &= \mathbf{O} \quad \text{in } V \\ \mathbf{D}\mathbf{k}\mathbf{D}^*\mathbf{u}_p + \mathbf{D}\boldsymbol{\sigma}_r + \mathbf{b} &= \mathbf{0} \quad \text{in } V \end{aligned} \tag{67}$$

The associated elastic stress fields (57) and (58) solve the corresponding Beltrami–Michell

equations, and are used to set up the approximation bases adopted in the hybrid–Trefftz stress model.

## 14. Computation of the finite element matrices

Because generalised variables are used, it is particularly simple to define sets of hierarchical functions to support the finite element stress, displacement and traction approximations. Moreover, the finite elements developed in this manner are not constrained to a particular geometry, as they may not be convex, simply connected or finite in dimension, and are sufficiently rich to produce accurate solutions when implemented on coarse meshes. Consequently, the pre-processing phase in the implementation of the finite element models presented above involves a relatively small data structure and is not strongly dependent on efficient meshing algorithms.

The hybrid–mixed formulations are the most flexible in what regards the choice of approximation functions, as they are not required to satisfy locally any of the elastodynamic conditions. To exploit best this feature in the computation of the finite element matrices, simple orthogonal, hierarchical functions should be used, namely digital Walsh functions and Wavelets, Legendre polynomials and trigonometric functions. When these functions are adopted, it becomes feasible to derive analytical expressions for the finite element matrices using the available symbolic programming codes, thus avoiding the implementation of numerical integration procedures. Reference to the implementation of these functions can be found in Freitas and Castro (1997) and Freitas et al. (1996).

The universe of the approximation functions available to implement the hybrid models is limited by the constraint to satisfy locally either the equilibrium or the compatibility condition. This limitation is stronger in the case of the hybrid–Trefftz formulation, which is based on solutions of the Helmholtz equation. The resulting approximation functions are more expensive to generate and, in general, only semi-analytical solutions may be established for the finite element matrices, leading to heavier numerical integration procedures.

The hybrid and the hybrid–Trefftz formulations enjoy the additional advantage of producing equilibrium and compatibility matrices with boundary integral expressions, a feature that in the hybrid–Trefftz formulation is extended to the elastodynamic matrix and all the stipulation vectors. The dimension of the problem is reduced in one order as in the boundary element method but without the disadvantages of loss of symmetry or the integration of singular fundamental solutions.

To improve the conditioning and the sparsity of the finite element solving systems, in all formulations and models, the domain approximation functions are referred to the principal axes of the element, with origin on its geometric centre. The same applies to the boundary approximation functions, with respect now to the corresponding boundary domain.

## 15. Processing of the finite element system

To assembly systems (36), (42) and (59) $\{$(37), (43) and (60)$\}$ for the displacement $\{$stress$\}$ model of the hybrid–mixed, hybrid and hybrid–Trefftz formulations, it suffices to enforce the same

traction approximation law (25) {displacement approximation law (28)} on the boundaries shared by connecting elements. The assembled systems thus obtained present the same general structure as the elementary systems they generate from. The summation of the contributions of connected elements typical of the conventional, displacement finite element formulation is replaced here by a direct allocation procedure.

In the stress model, the entries of vector $\mathbf{Q}_\Gamma$, which is associated with the interelement boundary tractions, are set to zero to model traction continuity. These entries are computed form definition (29) for the actually prescribed tractions on the assembled finite element mesh. Complementarily, in the displacement model, the entries of vector $\mathbf{v}_\Gamma$ are computed from definition (26) on the natural kinematic boundary of the finite element mesh and are set to zero on all interelement boundaries to model displacement continuity.

The sparse structure of the solving systems, enhanced by the high sparsity of the finite element matrices themselves, justifies the combination of sparse matrix storage schemes with the efficient, direct or iterative solvers for large systems now available, see e.g. Duff et al. (1986), Papadrakakis (1993) and Saad (1996). This is essential to overcome a major limitation of the hybrid–mixed formulation, that is its tendency to produce systems with a high number of degrees of freedom.

The second important limitation of the hybrid–mixed formulation is the possibility of linear dependency to emerge, leading to static or kinematic spurious modes. The schemes currently available to identify and deactivate a priori the existing spurious modes are too costly to implement. The simplest technique used to deal effectively with spurious modes consists in using weighing functions with a degree lower than that of the complementary field they are used to enforce and adapt the system solver to detect and delete the spurious modes that may persist.

It is stressed that the multiplicity of solutions that may be still exposed only affects a known subset of the variables. The unaffected field approximations, namely the stress field in the stress models or the displacement field in the displacement models, still produces reliable estimates, which can be be used to reconstruct the directly assumed field influenced by spurious modes.

These two major limitations of the hybrid–mixed formulation identified above should not affect the hybrid–Trefftz formulation. The strongly constrained approximation functions are linearly independent and the richness of the information they contain allows for accurate simulations using a relatively low number of degrees of freedom, in particular when they include the representation of local effects that are relevant for the convergence of the finite element approximation. The conditions that may cause spurious modes are analysed in Freitas (1997b), namely those deriving from the ill-balancing of the domain and boundary degrees of freedom.

The hybrid formulation is the best compromise in what concerns the strengths and weaknesses of the limiting hybrid–mixed and hybrid–Trefftz formulations. However, and as it is often the price of compromising, the hybrid formulation cannot attain the same levels of efficiency that typify each of the other two alternative approaches.

The solving systems it generates display sparsity indices and dimensions that are lower than those produced by the hybrid–mixed formulations but higher than the corresponding values found for the hybrid–Trefftz formulation. Unlike this formulation, the hybrid formulation is still susceptible to linear dependency. It is however possible to develop special macro-elements so designed as to keep the spurious modes in the set of internal variables and thus avoid their presence in the finite element solving system, Maunder et al. (1996).

## 16. Representation of the finite element solutions

The dynamic response of the structure is recovered by combining the solutions of the $n$-th order solving systems in any of the alternative formats stated in Tables 4, 7 and 9 for each of the approximations being implemented.

For instance, for the hybrid–mixed formulation, definitions (1), (9) and (20) produce the following expression for the estimate of the displacement field, where $\mathbf{u}_1$ is the solution of the forced vibration problem, $k$ is the order in the truncation of the time series, $\mathbf{q}_{2Vn}$ is the eigenvector and $\boldsymbol{\gamma}_n$ the corresponding amplitude in the $n$-th free vibration problem:

$$\mathbf{u} = \mathbf{u}_1 + \sum_{n=0}^{k} \mathbf{U}_{Vn}\mathbf{q}_{2Vn}\boldsymbol{\gamma}_n \, \mathrm{e}^{i\omega_{2n}t} \quad \text{in } V$$

$$\mathbf{u}_1 = \sum_{n=-k}^{+k} (\mathbf{U}_{Vn}\mathbf{q}_{1Vn} + \mathbf{u}_{pn}) \, \mathrm{e}^{i\omega_{1n}t} \quad \text{in } V$$

$$\boldsymbol{\gamma}_n = \boldsymbol{\alpha}_n \cos(\boldsymbol{\omega}_{2n}t) + \mathbf{i}\boldsymbol{\beta}_n \sin(\boldsymbol{\omega}_{2n}t) \tag{68}$$

The free vibration displacement amplitudes $\boldsymbol{\alpha}_n$ and $\boldsymbol{\beta}_n$ are determined using solution (68) to enforce the initial conditions (10) and (11) in the following weighed residual forms, where $\mathbf{u}_{10}$ and $\dot{\mathbf{u}}_{10}$ represent the initial conditions due to the forced vibration solution:

$$\int (\boldsymbol{\rho}_n \mathbf{U}_{Vn}\mathbf{q}_{2Vn})^t \left( \sum_{n=1}^{k} \mathbf{U}_{Vn}\mathbf{q}_{2Vn}\boldsymbol{\alpha}_n + \mathbf{u}_{10} - \mathbf{u}_0 \right) \mathrm{d}V = 0$$

$$\int (\boldsymbol{\rho}_n \mathbf{U}_{Vn}\mathbf{q}_{2Vn})^t \left( \sum_{n=1}^{k} i\boldsymbol{\omega}_{2n}\mathbf{U}_{Vn}\mathbf{q}_{2Vn}\boldsymbol{\beta}_n + \dot{\mathbf{u}}_{10} - \mathbf{u}_0 \right) \mathrm{d}V = 0$$

Using definition (B2) for the mass matrix and enforcing the orthogonality condition on the eigenvectors $\mathbf{q}_{2Vn}$, the systems above generate the following definitions for the free vibration modes:

$$\mathbf{q}_{2Vm}^t \mathbf{M}_{Vn}\mathbf{q}_{2Vn} = \boldsymbol{\delta}_{mn}\mathbf{A}_{mn}$$

$$A_{nn}\boldsymbol{\alpha}_n = \mathbf{q}_{2Vn}^t \int \mathbf{U}_{Vn}^t \boldsymbol{\rho}_n (\mathbf{u}_0 - \mathbf{u}_{10}) \, \mathrm{d}V$$

$$A_{nn}\boldsymbol{\omega}_{2n}(\mathbf{i}\beta_n) = \mathbf{q}_{2Vn}^t \int \mathbf{U}_{Vn}^t \boldsymbol{\rho}_n (\dot{\mathbf{u}}_0 - \dot{\mathbf{u}}_{10}) \, \mathrm{d}V$$

In the hybrid–mixed formulation, the stresses can be determined directly from the independent stress approximation defined by eqns (1), (9) and (19), to yield:

$$\boldsymbol{\sigma} = \boldsymbol{\sigma}_1 + \sum_{n=0}^{k} \mathbf{S}_{Vn}\mathbf{X}_{2Vn}\boldsymbol{\gamma}_n \, \mathrm{e}^{i\omega_{2n}t} \quad \text{in } V$$

$$\boldsymbol{\sigma}_1 = \sum_{n=-k}^{+k} (\mathbf{S}_{Vn}\mathbf{X}_{1Vn} + \boldsymbol{\sigma}_{pn}) \, \mathrm{e}^{i\omega_{1n}t} \quad \text{in } V \tag{69}$$

Similar expressions can be obtained for the boundary traction and displacement approximations (25) and (28), used, respectively, in the displacement and stress models of the hybrid–mixed formulation:

$$\mathbf{t} = \mathbf{t}_1 + \sum_{n=0}^{k} \mathbf{S}_{\Gamma n}\mathbf{X}_{2\Gamma n}\boldsymbol{\gamma}_n \, e^{i\omega_{2n}t} \quad \text{on } \Gamma_{\mathbf{u}} \tag{70}$$

$$\mathbf{u} = \mathbf{u}_1 + \sum_{n=0}^{k} \mathbf{U}_{\Gamma n}\mathbf{q}_{2\Gamma n}\boldsymbol{\gamma}_n \, e^{i\omega_{2n}t} \quad \text{on } \Gamma_{\boldsymbol{\sigma}}$$

$$\mathbf{t}_1 = \sum_{n=-k}^{+k} \mathbf{S}_{\Gamma n}\mathbf{X}_{1\Gamma n} \, e^{i\omega_{1n}t} \quad \text{on } \Gamma_{\mathbf{u}}$$

$$\mathbf{u}_1 = \sum_{n=-k}^{+k} \mathbf{U}_{\Gamma n}\mathbf{q}_{1\Gamma n} \, e^{i\omega_{1n}t} \quad \text{on } \Gamma_{\boldsymbol{\sigma}} \tag{71}$$

In the hybrid displacement model, the displacement field is computed from definition (68) and definition (70) is used to determine the boundary traction field. The stress field can be determined from the strains compatible with the displacement field (68), as it is the usual practice with conventional finite element formulations.

The stress field is the only domain field directly approximated in the hybrid stress model. The amplitudes of the free vibration modes can be determined using a weighed residual approach similar to that described above but applied now to the stress field definition (69), as stated in Appendix C. The displacements at points in the domain of the structure under analysis are determined either by integration of the estimate obtained for the stress field or, alternatively, using the equilibrium constraints (50)–(52). This limitation is not particularly relevant, as in most applications the information required from the analysis is limited to the boundary displacements, which can be directly computed from definition (71).

As for the hybrid models, in the hybrid–Trefftz models only one field is directly approximated in the domain, now with the added advantage that the stress, strain and displacement fields are directly related in consequence of enforcing directly the Helmholtz equation.

The methods described above to reconstruct the domain and boundary finite element approximations show that the post-processing phase can be implemented efficiently for all the formulations and models under discussion. The graphic representation of the finite element solutions is simplified because the field and boundary approximations are strictly element dependent and derive from linear combinations that can be efficiently processed using fast transform techniques. Moreover, smoothing techniques need not be applied as accurate solutions can be obtained using high degree, hierarchical approximation functions.

Also typical of all models under analysis is their suitability to parallel processing, Almeida and Freitas (1995). Besides being implemented on coarse meshes of super-elements, the high sparsity indices of the finite element solving systems are also consequent upon the low-level, highly localised element linkage. The generalised displacements and stresses, $\mathbf{q}_V$ and $\mathbf{X}_V$, used to describe the approximations in the domain of the elements are strictly element dependent. Similarly, the generalised tractions, $\mathbf{X}_\Gamma$, and displacements, $\mathbf{q}_\Gamma$, used in the displacement and stress models,

respectively, interact only with the elements directly connected to the boundary elements on which these variables are defined.

## 17. Numerical applications

The first set of tests is selected to illustrate the relative performance of the hybrid–mixed, hybrid and hybrid–Trefftz stress and displacement models. A simple, one-dimensional problem is chosen to limit to the essential the information to be assessed. With this simple application it is possible to illustrate the main features of the formulations being suggested, with the exception of all aspects directly related with the boundary conditions and approximations.

These aspects are analysed in the following two tests. An inappropriate basis is used to implement the hybrid displacement model in the free vibration analysis of the benchmark test on the tapered cantilever plate. The last application illustrates the representation of the displacement and stress fields developing in the forced vibration of a rectangular cantilever plate obtained with the displacement model of the hybrid–Trefftz formulation.

### *17.1. Vibration of a straight rod*

Let $L$ define the length of a straight rod with specific mass $\rho$ and Young modulus $E$. Assume that the body force and damping effects are neglected, so that the following equations,

$$\begin{aligned} \boldsymbol{\sigma}_x &= \Omega\rho\ddot{u} \\ \boldsymbol{\varepsilon} &= u_x \\ \boldsymbol{\sigma} &= E\boldsymbol{\varepsilon} \\ \boldsymbol{\sigma}(L,t) &= F(t) \\ u(0,t) &= 0 \end{aligned}$$

replace the fundamental elastodynamic conditions (4)–(8). In the equation above, $F(t)$ defines the forcing load per unit cross-section area, $\boldsymbol{\sigma}$, $\boldsymbol{\varepsilon}$, and $u$ denote the axial stress, strain and displacement fields, respectively, and subscript $x$ represents the partial derivative.

In this trivial one-dimensional application, the boundary approximation matrices present in definitions (25) and (28) reduce to forms (72) and (73), each being associated with a single degree of freedom, and implying that the corresponding boundary conditions are locally satisfied whenever they are explicitly enforced, as it happens in the displacement and stress models, respectively:

$$\mathbf{S}_{\Gamma n} = [1] \quad x = 0 \tag{72}$$

$$\mathbf{U}_{\Gamma n} = [1] \quad x = L \tag{73}$$

In the hybrid–mixed formulations, the approximations (19) and (20) for the axial stress $\boldsymbol{\sigma}$ and the displacement $u$ are based on orthogonal Legendre polynomials $P_m(\xi)$, with $\xi = 2x/L-1$:

$$\mathbf{S}_{Vn} = [P_0 \quad P_1 \quad \ldots \quad P_{n_x}] \quad 0 \leqslant x \leqslant L \tag{74}$$

$$\mathbf{U}_{Vn} = [P_0 \quad P_1 \quad \ldots \quad P_{n_q}] \quad 0 \leqslant x \leqslant L$$

$$P_0 = 1 \quad P_1 = \xi \quad P_2 = \tfrac{1}{2}(3\xi^2 - 1) \quad \ldots \tag{75}$$

The dimensions $n_X+1$ and $n_q+1$ of the vectors above define the number of degrees of freedom used in each approximation. In the context of one-dimensional analysis, to prevent the occurrence of spurious modes, it suffices to satisfy the conditions $n_X \leqslant n_q$ and $n_X \geqslant n_q$ in the implementation of the displacement and stress models, respectively. In this application, the particular solutions $\boldsymbol{\sigma}_p$ and $\mathbf{u}_p$ are set to zero. Due to the orthogonality of the approximation functions, the mass and the elasticity matrices are diagonal, and the domain equilibrium and compatibility matrices are also highly sparse.

The same approximation functions are used in the implementation of the hybrid stress and displacement models, where now only one of the approximations defined above is directly enforced. The dimension of the finite element solving system is substantially reduced but its sparsity index is lower because the dynamic matrix is not diagonal.

In the implementation of the hybrid–Trefftz formulation, the trigonometric solutions of the Helmholtz equation are used to approximate directly either the axial displacement or the stress,

$$\mathbf{U}_{Vn} = [\cos(\tfrac{1}{2}c\boldsymbol{\omega}_{in}\boldsymbol{\xi})\ \sin(\tfrac{1}{2}c\boldsymbol{\omega}_{in}\boldsymbol{\xi})]$$

$$\mathbf{S}_{Vn} = \frac{c}{L}\boldsymbol{\omega}_{in}\left[-\sin\left(\frac{1}{2}c\boldsymbol{\omega}_{in}\boldsymbol{\xi}\right)\cos\left(\frac{1}{2}c\boldsymbol{\omega}_{in}\boldsymbol{\xi}\right)\right]$$

where $c^2 = \rho L^2/E$. The dimension of the solving system is further reduced but its structure is similar to that of the hybrid formulations.

In the following presentation, the displacement approximation (75) {stress approximation (74)} is termed the primary approximation in the hybrid–mixed displacement {stress} model and the stress approximation (74) {displacement approximation (75)} is termed the secondary approximation in the same displacement {stress} model.

Summarised in Table 10 are the values obtained for the percent error, $\varepsilon_n$, in the estimates found for the natural frequencies with the hybrid–mixed and hybrid models using polynomials of degree $n$ in the primary approximation ($n = n_q$ for the displacement models and $n = n_X$ for the stress models) and degree $m = n-1$ in the secondary approximation ($m = n_X$ for the displacement models and $m = n_q$ for the stress models). Due to the nature of the application under consideration, the

Table 10
Percent error in the estimates for the natural frequencies computed with the hybrid–mixed and hybrid formulations

| $n$ | 1 | 2 | 3 | 4 | 5 |
|---|---|---|---|---|---|
| $\varepsilon_1$ | −10.269 | −0.376 | −0.006 | −0.000 | −0.000 |
| $\varepsilon_2$ | — | −20.380 | −2.633 | −0.256 | −0.017 |
| $\varepsilon_3$ | — | — | −33.015 | −6.067 | −1.082 |
| $\varepsilon_4$ | — | — | — | −48.277 | −10.717 |
| $\varepsilon_5$ | — | — | — | — | −65.247 |

hybrid–Trefftz stress and displacement models generate the correct estimates for the natural frequencies:

$$\omega_{2n} = (\tfrac{1}{2}+n)\pi c$$

Two distinct cases for the initial conditions are tested in the study of the vibration of the rod caused by a sinusoidal forcing load with maximum amplitude $F_0$ and frequency $\omega$. To avoid the activation of the free vibration modes, the initial conditions $u_0 = 0$ and $\dot{u}_0 = v$ are adopted in the first test case:

$$v(x) = \frac{F_0 L}{E\Omega}\frac{\sin(\omega c x/L)}{c\cos(\omega c)}$$

The hybrid–Trefftz models recover the solutions for the displacement and the axial stress:

$$u_1(x,t) = \frac{v}{\omega}\sin(\omega t)$$

$$\sigma_1(x,t) = Eu_{1x}$$

Also due to the particular nature of the application, the hybrid–mixed and hybrid formulations produce the same estimates for the same model, displacement and stress. The error in the estimates they generate is time independent, as they only mobilise the relevant term in the time series (9). The are registered in Tables 11 and 12, respectively, where the following index notation is used:

Table 11
Percent error in the estimates produced by the hybrid–mixed and hybrid displacement models

| $N$ | 1 | 2 | 3 | 4 | 5 |
|---|---|---|---|---|---|
| $\varepsilon_{\delta 0-V}$ | 0.0000 | 0.0000 | 0.0000 | 0.0000 | 0.0000 |
| $\varepsilon_{\delta L-V}$ | 1.1311 | 0.0683 | 0.0005 | 0.0000 | 0.0000 |
| $\varepsilon_{\sigma 0-V}$ | 10.987 | −4.7568 | −0.1313 | 0.0211 | 0.0003 |
| $\varepsilon_{\sigma L-V}$ | −25.884 | −6.3255 | 0.2444 | 0.0287 | 0.0006 |
| $\varepsilon_{\sigma 0-\Gamma}$ | 1.8354 | 0.0201 | 0.0009 | 0.0000 | 0.0000 |

Table 12
Percent error in the estimates produced by the hybrid–mixed and hybrid stress models

| $n$ | 1 | 2 | 3 | 4 | 5 |
|---|---|---|---|---|---|
| $\varepsilon_{\delta 0-V}$ | 0.5082 | 0.0277 | 0.0042 | 0.0001 | 0.0000 |
| $\varepsilon_{\delta L-V}$ | 50.566 | −3.2165 | −0.5070 | 0.0134 | 0.0013 |
| $\varepsilon_{\sigma 0-V}$ | 1.8354 | 0.0201 | 0.0009 | 0.0000 | 0.0000 |
| $\varepsilon_{\sigma L-V}$ | 0.0000 | 0.0000 | 0.0000 | 0.0000 | 0.0000 |
| $\varepsilon_{\delta L-\Gamma}$ | 6.2134 | 0.0120 | 0.0003 | 0.0000 | 0.0000 |

- $\varepsilon_{\delta 0-V}$ and $\varepsilon_{\delta L-V}$ denote the percent error in the estimate obtained from the domain approximation of the axial displacement at points $x = 0$ and $x = L$, respectively;
- $\varepsilon_{\sigma 0-V}$ and $\varepsilon_{\sigma L-V}$ denote the percent error in the estimate obtained from the domain approximation of the axial stress at the same points;
- in the displacement models, $\varepsilon_{\sigma 0-\Gamma}$ represents the percent error in the estimate of the axial stress at boundary $x = 0$ and, in the stress models, $\varepsilon_{\delta 0-\Gamma}$ represents the percent error in the estimate of the axial displacement at boundary $x = L$, as computed from the corresponding boundary approximations.

Because the complementary boundary condition is explicitly enforced, the displacement {stress} models recover the exact solution for the displacement at $x = 0$ {stress at $x = L$} in this one-dimensional application.

The results summarised in Tables 11 and 12 display patterns of convergence similar to those that have been found using the same formulations and models in the solution of quasi-static, elastic and elastoplastic problems:

- Convergence is not necessarily monotonic;
- The boundary approximations present a better convergence rate than that of the corresponding estimate produced by the domain approximation;
- In the hybrid–mixed models, the estimates for the primary approximation field converge faster than the estimates for the secondary approximation field, meaning that the displacement {stress} models should be used when emphasis is placed on the precision of the solution found for the displacements {stresses};
- The hybrid models can produce solutions with the same level of accuracy as those obtained from the primary approximation in the corresponding hybrid–mixed model using, however, substantially fewer degrees of freedom. The same comment applies to the direct comparison of the hybrid–Trefftz and hybrid models.

The values presented in Tables 13, 14 and 15 illustrate the importance of the role played by the secondary approximation field in the estimates computed with the hybrid–mixed displacement and stress models, respectively, identified as the HMD and HMS models.

In the hybrid—mixed displacement {stress} model, the degree of the primary displacement {stress} approximation is fixed and set to the fifth degree, $n = 5$, and the degree $m$ of the secondary stress {displacement} approximation ranges from 0 to $n-1$.

Table 13
Effect of the secondary approximation in the estimates for the natural frequencies (HMD and HMS models with $n = 5$)

| $m$ | 0 | 1 | 2 | 3 | 4 |
|---|---|---|---|---|---|
| $\varepsilon_1$ | −276.649 | −8.582 | −0.248 | −0.006 | −0.000 |
| $\varepsilon_2$ | — | −146.350 | −12.979 | −1.583 | −0.017 |
| $\varepsilon_3$ | — | — | −115.635 | −13.846 | −1.082 |
| $\varepsilon_4$ | — | — | — | −82.191 | −10.717 |
| $\varepsilon_5$ | — | — | — | — | −65.247 |

Table 14
Effect of the secondary approximation in the estimates computed with the hybrid–mixed displacement model ($n = 5$)

| $m$ | 0 | 1 | 2 | 3 | 4 |
|---|---|---|---|---|---|
| $\varepsilon_{\delta 0-V}$ | 0.0000 | 0.0000 | 0.0000 | 0.0000 | 0.0000 |
| $\varepsilon_{\delta L-V}$ | 20.051 | 5.3800 | 0.0078 | 0.0002 | 0.0000 |
| $\varepsilon_{\sigma 0-V}$ | 28.021 | 0.9093 | −0.0329 | 0.0085 | 0.0003 |
| $\varepsilon_{\sigma L-V}$ | −1.7940 | −0.8125 | 0.0876 | 0.0108 | 0.0006 |
| $\varepsilon_{\sigma 0-\Gamma}$ | 27.809 | 1.5859 | 0.0130 | 0.0001 | 0.0000 |

Table 15
Effect of the secondary approximation in the estimates computed with the hybrid–mixed stress model ($n = 5$)

| $m$ | 0 | 1 | 2 | 3 | 4 |
|---|---|---|---|---|---|
| $\varepsilon_{\delta 0-V}$ | −0.0264 | 0.0015 | 0.0000 | 0.0000 | 0.0000 |
| $\varepsilon_{\delta L-V}$ | 97.335 | 0.4164 | −0.1353 | 0.0060 | 0.0013 |
| $\varepsilon_{\sigma 0-V}$ | 27.809 | 1.5859 | 0.0130 | 0.0001 | 0.0000 |
| $\varepsilon_{\sigma L-V}$ | 0.0000 | 0.0000 | 0.0000 | 0.0000 | 0.0000 |
| $\varepsilon_{\delta L-\Gamma}$ | 94.709 | 0.9652 | 0.0442 | 0.0000 | 0.0000 |

In the second test case, homogeneous initial conditions, $u_0 = 0$ and $\dot{u}_0 = 0$, are chosen to mobilise the free vibration modes. To model the beating effect by excitation of the fundamental vibration mode, the frequency of the forcing load is set to 80 Hz, by letting $c = 0.02$ s. The hybrid–Trefftz stress and displacement models generate the correct series solutions for this application:

$$\boldsymbol{\sigma}(x,t) = \boldsymbol{\sigma}_1(x,t) - 2F_0 \frac{\boldsymbol{\omega}}{c} \sum_{n=1}^{\infty} \frac{\sin(\boldsymbol{\omega}_{2n} c)}{(\boldsymbol{\omega}_{2n}^2 - \boldsymbol{\omega}^2)} \sin(\boldsymbol{\omega}_{2n} t) \cos(\boldsymbol{\omega}_{2n} cx/L)$$

$$u(x,t) = u_1(x,t) - 2F_0 \frac{\boldsymbol{\omega} L}{Ec^2} \sum_{n=1}^{\infty} \frac{\sin(\boldsymbol{\omega}_{2n} c)}{(\boldsymbol{\omega}_{2n}^2 - \boldsymbol{\omega}^2)\boldsymbol{\omega}_{2n}} \sin(\boldsymbol{\omega}_{2n} t) \sin(\boldsymbol{\omega}_{2n} cx/L)$$

Shown in Fig. 1 is the envelope found for the non-dimensional displacement $\delta = Eu/F_0 L$ at the free end of the rod, $x = L$.

In the remaining illustrations, the abbreviation HMD($n_q, n_X$) is used to identify the solutions obtained with the hybrid–mixed displacement model based on polynomials of degree $n_q - 1$ and $n_X - 1$ to approximate the displacement and axial force fields, respectively. The corresponding notation for the stress model is HMS($n_X, n_q$) and the abbreviations HD($n_q$) and HS($n_X$) identify the solutions derived from the hybrid displacement and stress models, respectively.

The estimate produced by the hybrid–mixed stress model HMS(3, 2) for the displacement at the fixed end of the rod, $x = 0$, using a quadratic approximation for the axial force field ($n_X = 3$) and

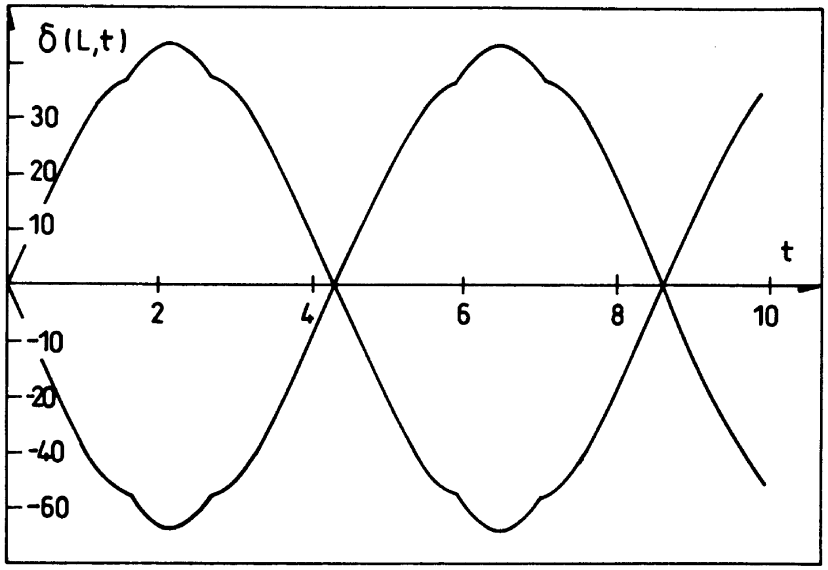


Fig. 1. Envelope of the variation of the displacement at $x = L$, obtained with the hybrid–Trefftz solution (time in seconds).

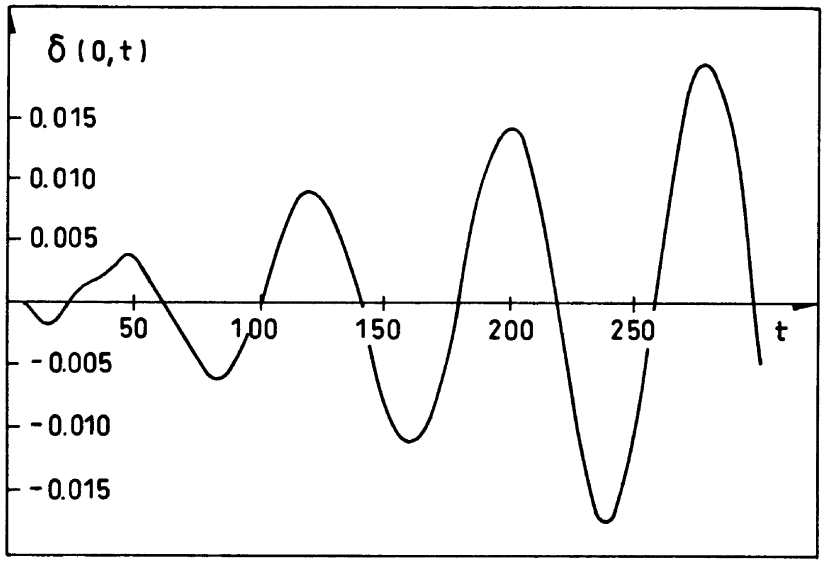


Fig. 2. Displacement at $x = 0$ determined with the HMS(3, 2) model (time in millisecond).

a linear approximation for the displacement field ($n_q = 2$) is shown in Fig. 2. The kinematic boundary condition is satisfactorily satisfied for this low level approximation.

The variation with time of the displacement computed at the free end with the different for-

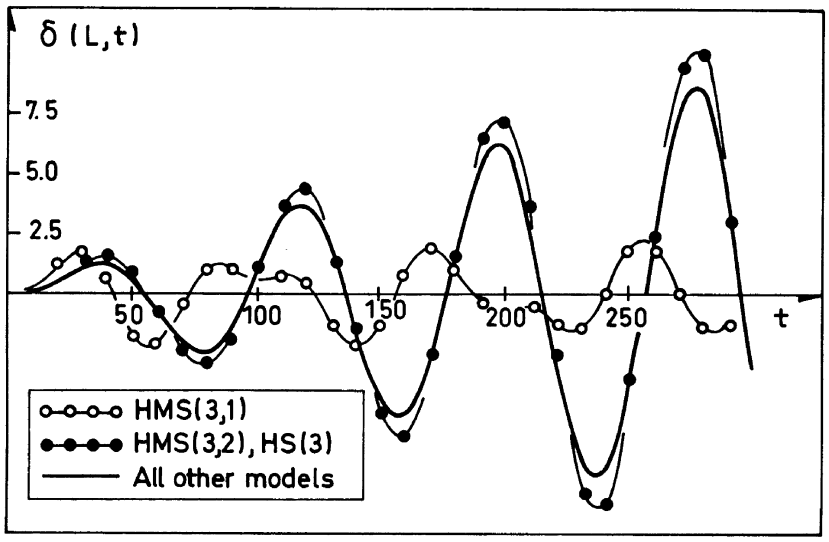


Fig. 3. Displacement at $x = L$ determined with the alternative models (time in millisecond).

mulations and models is shown in Fig. 3. It is seen that the hybrid–mixed and hybrid displacement models HMD(3, 2) and HD(3) approximate well the Trefftz solution. The importance of the role played by the secondary approximation in the convergence of the solutions is again clearly illustrated by the solutions obtained with the stress models.

The displacement estimates shown for these models are those produced directly by the displacement approximation, which is constant and linear, respectively, for the solutions HMS(3, 1) and HMS(3, 2). The solution of the hybrid stress model HS($n_X$) is equivalent to the solution obtained with the corresponding hybrid–mixed stress model with the highest possible secondary field approximation, HMS($n_X, n_X - 1$).

As it is shown in Fig. 4, this same pattern is repeated for the estimates obtained for the axial force at the fixed end of the rod. Parameter $v = \sigma/F_0$ defines the non-dimensional axial stress. The Trefftz solution is now satisfactorily approximated by the hybrid–mixed and hybrid stress models, while the solutions obtained with the hybrid–mixed displacement model converge to the corresponding hybrid displacement estimates.

Figure 5 is presented to illustrate the combined influence of the approximations in the initial and boundary conditions. Because the static boundary condition is enforced and satisfied by the stress models, the solutions they produce recover the Trefftz estimates. As this condition is not directly enforced by the displacement model, the hybrid and hybrid–mixed solutions are affected by the initial, zero-velocity condition, which does not influence, however, the hybrid–Trefftz displacement solution.

### *17.2. Free vibration of tapered cantilever plate*

The tapered cantilever shown in Fig. 6 is a test recommended by NAFEMS (1990). It is used here to illustrate the *h*-refinement convergence of the eigen-solutions obtained with the hybrid

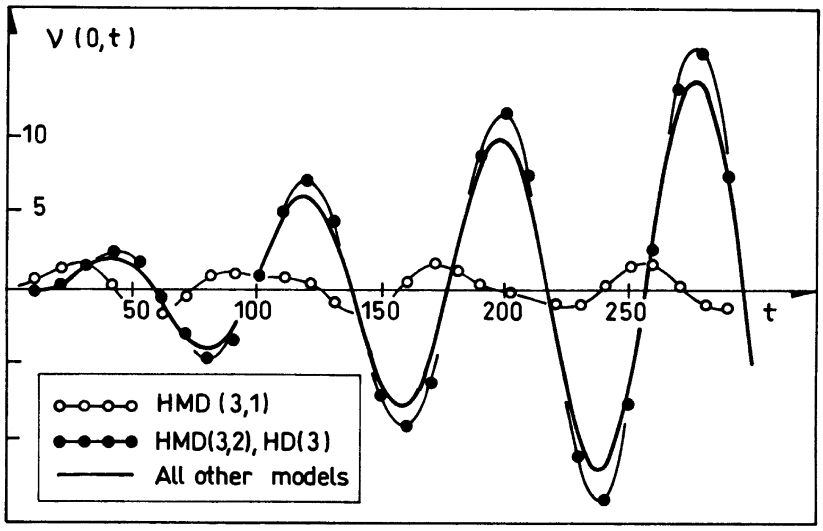


Fig. 4. Axial stress at $x = 0$ determined with the alternative models (time in millisecond).

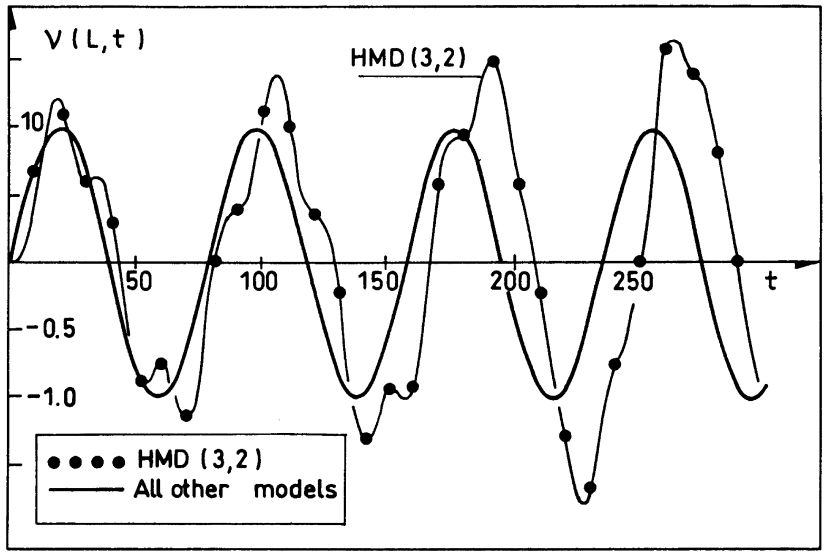


Fig. 5. Axial stress at $x = L$ determined with the alternative models (time in millisecond).

displacement model when an inadequate approximation basis is used. This basis is taken as the solution of the Navier eqn (67), with a displacement field of degree 10 derived from the harmonic potential $\varphi = r^n e^{in\theta}$, in polar co-ordinates $(r, \theta)$.

The associated stress distribution induces a trivial inertia force field, in consequence of the static equilibrium condition (66). Fourth degree polynomials are used to approximate the tractions on the interelement boundaries of the four finite element meshes shown in Fig. 6 and, also, on the

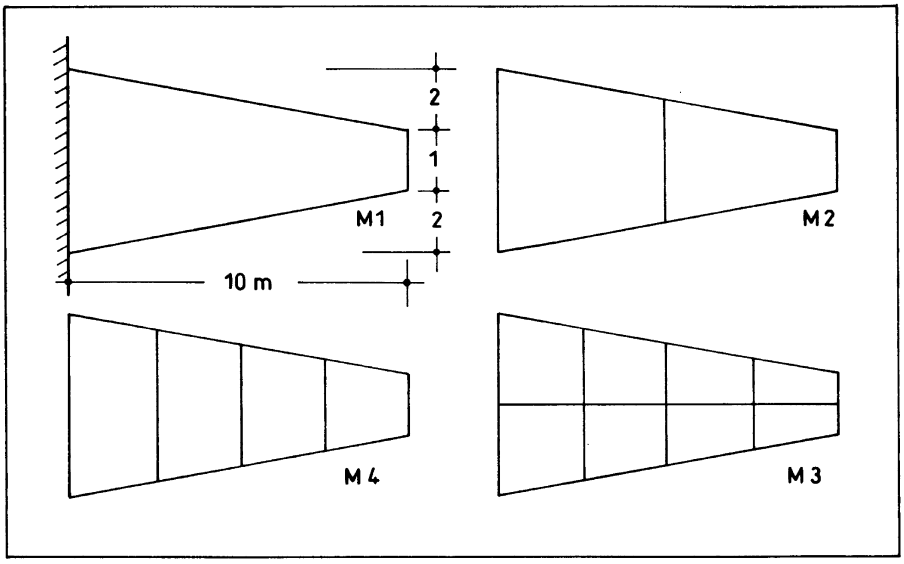


Fig. 6. The tapered cantilever test.

kinematic boundary of the plate. The thickness of the plate is $t = 0.05$ mm and the material constants are the following: $E = 200$ GPa, $\rho = 8000$ kg/m$^3$, $v = 0.3$.

The estimates obtained for the first six natural frequencies, normalised to the solutions of NAFEMS, are given in Table 16 and the corresponding mode shapes are shown in Fig. 7. They compare acceptably well with the results obtained with the ABAQUS (1994) code using a $16 \times 8$ mesh built with the following elements: the standard four- and eight-node elements, CPS4 and CPS8, the four-node element with an incompatible node, CPS4i, and the eight-node element with reduced integration, CPS8I.

It is noted that the simulation of free vibration with hybrid–Trefftz elements leads to implicit eigenvalue problems only by specific design, and may not be the most efficient approach to

Table 16
Normalised natural frequencies for the tapered cantilever test

| | Hybrid displacement model | | | | ABAQUS | | | |
|---|---|---|---|---|---|---|---|---|
| Mode | Mesh 1 | Mesh 2 | Mesh 3 | Mesh 4 | CPS4 | CPS4i | CPS8 | CPS8i |
| 1 | 1.0006 | 1.0002 | 1.0001 | 1.0000 | 1.0036 | 0.9978 | 1.0003 | 1.0001 |
| 2 | 1.0079 | 1.0058 | 1.0032 | 0.9999 | 1.0046 | 0.9963 | 1.0009 | 1.0006 |
| 3 | 1.0233 | 1.0126 | 1.0041 | 1.0030 | 0.9993 | 0.9991 | 1.0001 | 1.0000 |
| 4 | 1.0308 | 1.0292 | 1.0130 | 1.0054 | 1.0030 | 0.9922 | 1.0024 | 1.0015 |
| 5 | 1.0688 | 1.0554 | 1.0296 | 1.0137 | 0.9980 | 0.9857 | 1.0056 | 1.0037 |
| 6 | 1.1418 | 1.0961 | 1.0254 | 1.0204 | 0.9959 | 0.9953 | 1.0003 | 1.0002 |

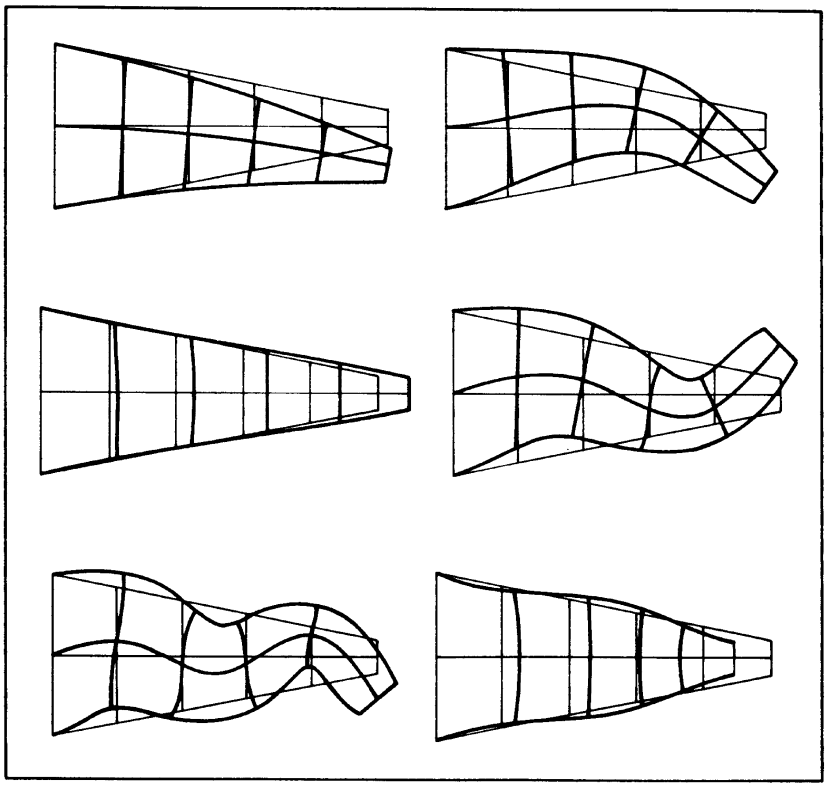

Fig. 7. The first six eigenmodes of the tapered cantilever.

determine natural frequencies and vibration modes. Indeed, the eigenvalue problem can be solved as for any other finite element formulation, simply by replacing the dynamic matrix in the solving system by the equivalent definitions (61) and (64), for the displacement and stress models, respectively.

### *17.3. Forced vibration of a rectangular cantilever plate*

The displacement model of the hybrid–Trefftz formulation is applied to simulate the response of a rectangular cantilever by the periodic, uniform forcing load shown in Fig. 8. The wave solutions of the governing Helmholtz eqn (58) are derived from potentials of the following form, where $J_n$ is the Bessel function of the first kind and order $n$,

$$\varphi = J_n(kr)\,\mathrm{e}^{in\theta}$$

$k^2 = \rho\omega^2/G$ and $k^2 = (1-2\nu)\rho\omega^2/2(1-\nu)G$ for the shear and longitudinal modes, respectively, with $G$ representing the shear modulus and $\omega$ the frequency of the sinusoidal forcing load. The material constants used are $E = 206$ GPa and $\rho = 7500$ kg/m$^3$ and all results presented below are determined at instant $t = \pi/2\omega$.

The cantilever beam is a particularly difficult test case for the displacement model when coarse

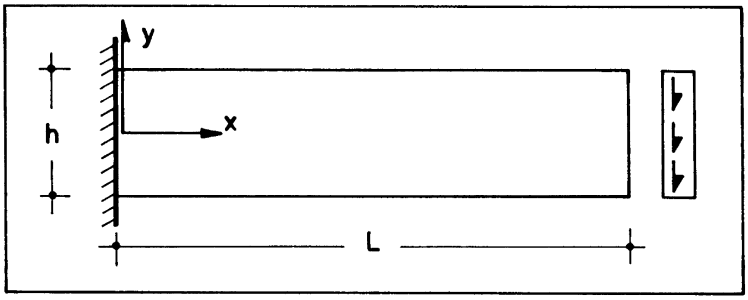


Fig. 8. The rectangular cantilever test.

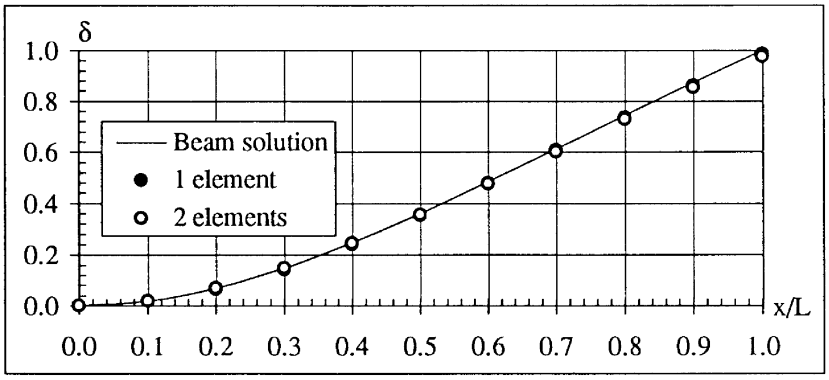


Fig. 9. Displacement estimates ($L/h = 10$).

finite element meshes are used, as the only continuity conditions that are directly enforced by this model are the clamped-end conditions and the interelement displacement continuity conditions. The static and interelement stress continuity conditions are not explicitly enforced, meaning that in the cantilever test relatively weaker estimates for the stress components should be expected.

The plate is first solved with the aspect ratio $L/h = 10$, $\omega = 700$ rad/s and $v = 0$ to test the ability of the model to recover the beam theory solution. The estimates obtained for the displacement, bending moment and shear force distributions are shown in Figs 9–11, scaled to the maximum beam solutions, namely $\delta = u(x)/u(L)$, $m = M(x)/M(0)$, $v = V(x)/V(0)$.

It is seen that the single element mesh, with 26 degrees of freedom in the domain displacement approximation and 10 degrees of freedom in the boundary traction approximation, produces good estimates only for the displacement and bending moment distributions. The estimate for the shear force distribution improves substantially when the slender beam is solved with two elements, with an improved aspect ratio and the same number of degrees of freedom per element. The differences found near the clamped end of the beam are caused by stress distributions that the beam theory solution cannot model correctly.

The same test is run with aspect ratio $L/h = 2$, $\omega = 3000$ Hz and $v = 0.3$. The estimates obtained with a two-element mesh are given in Fig. 12. The degrees of freedom per domain and boundary

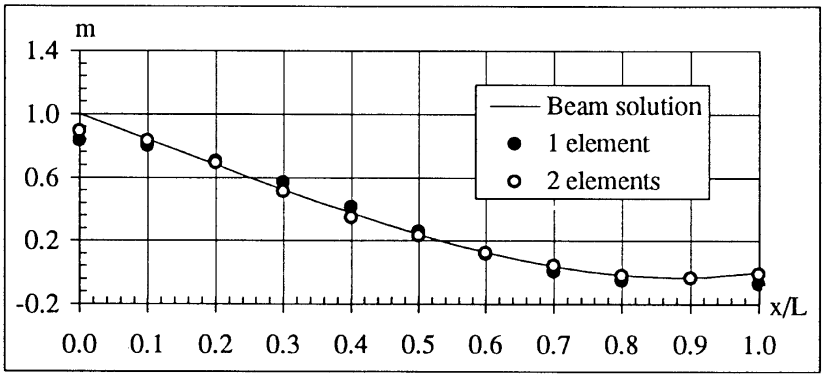


Fig. 10. Bending moment estimates ($L/h = 10$).

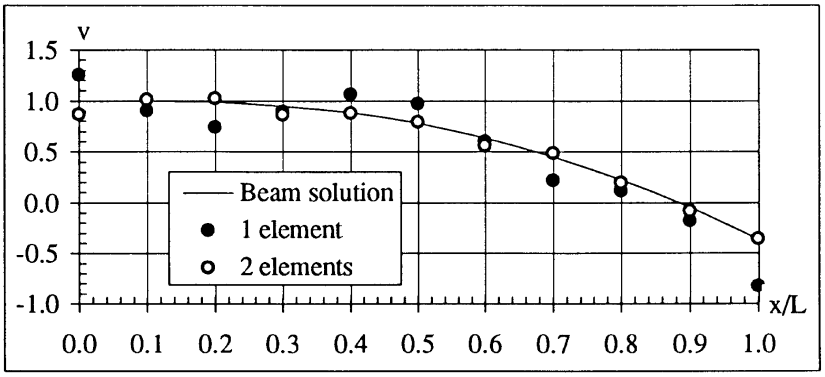


Fig. 11. Shear force estimates ($L/h = 10$).

element are 38 and 16, respectively. These results are directly computed from the finite element displacement approximation in the domain of the elements. No smoothing is used in the representation of displacement and associated stress fields. The limit values used in the (red–blue) colour scales for the stress components, scaled to the forcing load, are the following: $\sigma_{xx}$: $(-3; +3)$, $\sigma_{yy}$: $(-0.75; +0.75)$ and $\sigma_{xy}$: $(-1.5; +1.5)$. Light green corresponds to the zero of the colour scale.

As for the slender beam tests, the deflected shape shows that the displacement continuity and boundary conditions are strongly enforced. The simulation of these conditions on the stress components is weaker because they are not explicitly enforced and also due to the coarse mesh being used. The defective estimates concentrate mainly on the interelement shear stress continuity condition and on the static boundary conditions in the vicinity of the clamped end. This is consequent upon the fact that the approximation used does not include the singular terms necessary to model correctly the stresses in the neighbourhood of the corner points.

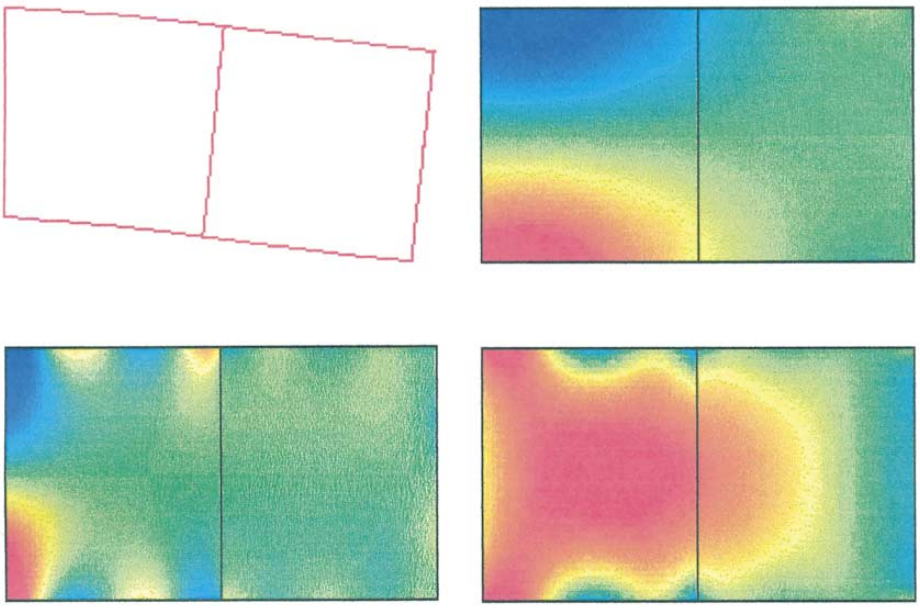

Fig. 12. Displacement and stress distributions $\boldsymbol{\sigma}_{xx}$, $\boldsymbol{\sigma}_{yy}$, and $\boldsymbol{\sigma}_{xy}$.

## 18. Closure

The structure and the contents of this paper are so chosen as to present, in a necessarily compact form, a global view of the alternative hybrid finite element formulations and models for the spectral analysis of linear elastodynamic problems.

Despite their simplicity, the tests used to illustrate the implementation of the formulations and models being suggested can expose the most relevant patterns of convergence and performance. These are found to be in agreement with the experience accumulated using the same formulations and models in the elastic and elastoplastic quasi-static analysis of laminar structures and solids.

Because they are not built on the node concept, all three formulations can accommodate very easily the simulation of local effects, namely the singular solutions associated with cracks or point loads. Also, they are equally and particularly well suited to be implemented with adaptive procedures and in a parallel processing mode, as the approximation bases are strongly element dependent and naturally hierarchical.

As it is well known, these features are not particular to the formulations and models discussed here. They can be built into any mixed or hybrid finite element, including the Trefftz variants. What is particular of the approach is the extensive, full use of generalised variables to allow *p*-refinement to act independently in each finite element or on each boundary element. The price paid is the necessity of producing special purpose computer programmes, thus hindering one of the most effective ways to generalise the use of hybrid elements, namely their emulation as conforming elements, frequently offered in the libraries of the commercial codes based on conventional displacement elements.

In contrast with the hybrid–mixed formulation and, to a lesser extent, with the hybrid formulation, the generalisation of the hybrid–Trefftz variant to non-linear problems can be quite demanding. Yet another relative weakness of the hybrid–Trefftz formulation is the comparative higher cost involved in the computation of the finite element structural arrays, as it cannot benefit from the freedom offered by the hybrid–mixed formulation in the selection of computer-tailored approximation bases, leading to highly sparse solving systems and to the explicit derivation of the expressions of the finite element structural arrays using the now widely available symbolic manipulation codes.

The comments made above may discourage the usual temptation to enthrone a particular combination of model and formulation, as this selection is often very much problem and machine dependent.

## Acknowledgements

The author wishes to thank the reviewers for their suggestions to improve the objectivity, clarity and accuracy of the text. The author wishes also to thank C. Cismasiu, I. Farasyn and J. Maeck for the plate stretching applications and Prof. G. De Roeck, Catholic University of Leuven, Belgium, for his suggestion to extend to elastodynamic problems the hybrid finite element formulations previously developed for quasi-static structural analysis applications. This work is part of the research developed at ICIST, Instituto Superior Técnico, and has been supported by Junta Nacional de Investigação Científica e Tecnológica, through project PRAXIS/2/2.1/CEG/33/94.

## Appendix A: Time discretization

The average enforcement of the dynamic equilibrium condition (4) for the Fourier time basis is,

$$\int_0^T \mathrm{e}^{-i\omega_{jn}t}(\mathbf{D}\boldsymbol{\sigma}_j + \boldsymbol{\delta}_{j1}\mathbf{b})\,\mathrm{d}t = \int_0^T \mathrm{e}^{-i\omega_{jn}t}(\mathbf{d}\dot{\mathbf{u}}_j + \boldsymbol{\rho}\ddot{\mathbf{u}}_j)\,\mathrm{d}t$$

with $\omega_{jn} = 2n\pi/T$. Integration by parts of the equation above yields:

$$\int_0^T \mathrm{e}^{-i\omega_{1n}t}(\mathbf{D}\boldsymbol{\sigma}_j + \boldsymbol{\rho}_{jn}\boldsymbol{\omega}_{jn}^2\mathbf{u}_j + \boldsymbol{\delta}_{j1}\mathbf{b})\,\mathrm{d}t = [\mathrm{e}^{-i\omega_{jn}t}(\mathbf{d}\mathbf{u}_j + \boldsymbol{\rho}\dot{\mathbf{u}}_j + \mathbf{i}\boldsymbol{\omega}_{jn}\boldsymbol{\rho}\mathbf{u}_j)]_0^T$$

Result (11) is recovered by enforcing definition (10) in the equation above and assuming that $T$ represents the actual or the fictitious period of the response: $\mathbf{u}_1(\mathbf{x},0) = \mathbf{u}_1(\mathbf{x},T)$ and $\dot{\mathbf{u}}_1(\mathbf{x},0) = \dot{\mathbf{u}}_1(\mathbf{x},T)$. Equation (13) is obtained in a similar manner.

## Appendix B: Definition of the finite element arrays

Hybrid–mixed displacement model

Equilibrium and compatibility matrices:

$$\mathbf{B}_{Vn} = \int (\mathbf{D}^*\mathbf{U}_{Vn})^t\mathbf{S}_{Vn}\,\mathrm{d}V$$

$$\mathbf{B}_{\Gamma n} = \int \mathbf{U}_{Vn}^t\mathbf{S}_{\Gamma n}\,\mathrm{d}\Gamma_{\mathbf{u}}$$

Flexibility and mass matrices:

$$\mathbf{F}_{Vn} = \int \mathbf{S}_{Vn}^t\mathbf{f}_n\mathbf{S}_{Vn}\,\mathrm{d}V \tag{B1}$$

$$\mathbf{M}_{Vn} = \int \mathbf{U}_{Vn}^t\boldsymbol{\rho}_n\mathbf{U}_{Vn}\,\mathrm{d}V \tag{B2}$$

Prescribed displacements and strains:

$$\mathbf{v}_{pn} = \int \mathbf{S}_{\Gamma n}^t\mathbf{u}_{pn}\,\mathrm{d}\Gamma_{\mathbf{u}}$$

$$\mathbf{e}_{pn} = \int \mathbf{S}_{Vn}^t\mathbf{D}^*u_{pn}\,\mathrm{d}V$$

$$\mathbf{e}_{0n} = \int \mathbf{S}_{Vn}^{t}(\boldsymbol{\varepsilon}_{rn} + \mathbf{f}_{n}\boldsymbol{\sigma}_{pn})\,\mathrm{d}V$$

Prescribed tractions and inertia forces:

$$\mathbf{Q}_{tn} = \int \mathbf{U}_{Vn}^{t}\mathbf{t}_{\Gamma n}\,\mathrm{d}\Gamma_{\sigma}$$

$$\mathbf{Q}_{pn} = \int \mathbf{U}_{Vn}^{t}\mathbf{D}\boldsymbol{\sigma}_{pn}\,\mathrm{d}V \tag{B3}$$

$$\mathbf{Q}_{fn} = \omega_{n}^{2}\int \mathbf{U}_{Vn}^{t}\boldsymbol{\rho}_{n}\mathbf{u}_{pn}\,\mathrm{d}V \tag{B4}$$

Stipulation vectors in governing system:

$$\begin{aligned}\mathbf{f}_{Vn} &= \mathbf{Q}_{bn} + \mathbf{Q}_{tn} - \mathbf{Q}_{pn} - \mathbf{Q}_{fn}\\ \mathbf{d}_{Vn} &= \mathbf{e}_{0n} - \mathbf{e}_{pn}\\ \mathbf{d}_{\Gamma n} &= \mathbf{v}_{pn} - \mathbf{v}_{\Gamma n}\end{aligned} \tag{B5}$$

Hybrid displacement model

Stiffness matrix and prescribed stresses:

$$\mathbf{K}_{Vn} = \int \mathbf{E}_{Vn}^{t}\mathbf{k}_{n}\mathbf{E}_{Vn}\,\mathrm{d}V \tag{B6}$$

$$\mathbf{X}_{0n} = \int \mathbf{E}_{Vn}^{t}(\boldsymbol{\sigma}_{rn} + \mathbf{k}_{n}\boldsymbol{\varepsilon}_{pn})\,\mathrm{d}V \tag{B7}$$

Stipulation vectors in governing system:

$$\mathbf{f}_{Vn} = \mathbf{Q}_{bn} + \mathbf{Q}_{fn} + \mathbf{Q}_{tn} - \mathbf{X}_{0n} \tag{B8}$$

Definition (B5) holds.

Hybrid–mixed stress model

Equilibrium and compatibility matrices:

$$\mathbf{A}_{Vn} = \int (\mathbf{D}\mathbf{S}_{Vn})^{t}\mathbf{U}_{Vn}\,\mathrm{d}V$$

$$\mathbf{A}_{\Gamma n} = \int (\mathbf{N}\mathbf{S}_{Vn})^{t}\mathbf{U}_{\Gamma n}\,\mathrm{d}\Gamma_{\sigma}$$

Prescribed generalised strains:

$$\mathbf{e}_{\Gamma n} = \int (\mathbf{N}\mathbf{S}_{Vn})^t \mathbf{u}_{\Gamma n}\, \mathrm{d}\Gamma_{\mathbf{u}}$$

$$\mathbf{e}_{pn} = \int (\mathbf{D}\mathbf{S}_{Vn})^t \mathbf{u}_{pn}\, \mathrm{d}V$$

Prescribed tractions and inertia forces:

$$\mathbf{Q}_{tn} = \int \mathbf{U}_{\Gamma n}^t \mathbf{N}\boldsymbol{\sigma}_{pn}\, \mathrm{d}\Gamma_{\boldsymbol{\sigma}}$$

Definitions (B3) and (B4) hold.

Stipulation vectors in governing system:

$$\begin{aligned} \mathbf{d}_{Vn} &= \mathbf{e}_{\Gamma n} - \mathbf{e}_{pn} - \mathbf{e}_{0n} \\ \mathbf{f}_{Vn} &= -\mathbf{Q}_{bn} - \mathbf{Q}_{pn} - \mathbf{Q}_{fn} \\ \mathbf{f}_{\Gamma n} &= \mathbf{Q}_{\Gamma n} - \mathbf{Q}_{tn} \end{aligned} \tag{B9}$$

Hybrid stress model

Mobility matrix and prescribed strains:

$$\tilde{\mathbf{M}}_{Vn} = \int (\mathbf{D}\mathbf{S}_{Vn})^t \boldsymbol{\rho}_n^{-1} (\mathbf{D}\mathbf{S}_{Vn})\, \mathrm{d}V \tag{B10}$$

$$\mathbf{e}_{un} = \boldsymbol{\omega}_n^{-2} \int (\mathbf{D}\mathbf{S}_{Vn})^t \boldsymbol{\rho}_n^{-1} (\mathbf{b}_n + \mathbf{D}\boldsymbol{\sigma}_{pn})\, \mathrm{d}V \tag{B11}$$

Stipulation vectors in governing system:

$$\mathbf{d}_{Vn} = \mathbf{e}_{\Gamma n} + \mathbf{e}_{un} - \mathbf{e}_{0n} \tag{B12}$$

Definition (B9) holds.

## Appendix C: Representation of the finite element solution

The amplitudes of the free vibration modes are determined from the following weighed residual statements, where $\boldsymbol{\sigma}_0$ and $\dot{\boldsymbol{\sigma}}_0$ represent the stresses and the stress gradients computed from the initial displacement and velocity fields $\mathbf{u}_0$ and $\dot{\mathbf{u}}_0$, respectively:

$$\int (\mathbf{f}_n \mathbf{S}_{Vn} \mathbf{X}_{2Vn})^t \left( \sum_{n=1}^{k} \mathbf{S}_{Vn} \mathbf{X}_{2Vn} \boldsymbol{\alpha}_n + \boldsymbol{\sigma}_{10} - \boldsymbol{\sigma}_0 \right) \mathrm{d}V = 0$$

$$\int (\mathbf{f}_n \mathbf{S}_{Vn} \mathbf{X}_{2Vn})^t \left( \sum_{n=1}^{k} i\boldsymbol{\omega}_{2n} \mathbf{S}_{Vn} \mathbf{X}_{2Vn} \boldsymbol{\beta}_n + \dot{\boldsymbol{\sigma}}_{10} - \dot{\boldsymbol{\sigma}}_0 \right) \mathrm{d}V = 0$$

The following definitions result from the enforcement of the $\mathbf{F}_{Vn}$-orthogonality condition:

$$\mathbf{B}_{nn} \boldsymbol{\alpha}_n = \mathbf{X}_{2Vn}^t \int \mathbf{S}_{Vn}^t \mathbf{f}_n (\boldsymbol{\sigma}_0 - \boldsymbol{\sigma}_{10}) \, \mathrm{d}V$$

$$\mathbf{B}_{nn} \boldsymbol{\omega}_{2n} (i\boldsymbol{\beta}_n) = \mathbf{X}_{2Vn}^t \int \mathbf{S}_{Vn}^t \mathbf{f}_n (\dot{\boldsymbol{\sigma}}_0 - \dot{\boldsymbol{\sigma}}_{10}) \, \mathrm{d}V$$

$$\mathbf{X}_{2Vm}^t \mathbf{F}_{Vn} \mathbf{X}_{2Vn} = \boldsymbol{\delta}_{mn} \mathbf{B}_{mn}.$$

## References


ABAQUS, 1994. Verification Manual, version 5.4, Hibbit, Karlsson and Sorensen, Inc.

Almeida, J.P.M., Freitas, J.A.T., 1995. On the parallel implementation of non-conventional finite element formulations. In: Papadrakakis, M. (Ed.), Advanced Finite Element Solution Techniques. CIMNE.

Almeida, J.P.M., Pereira, O.J.B.A., 1996. A set of hybrid equilibrium finite element models for the analysis of three-dimensional solids. Int. J. Numer. Meth. Engng 39, 2789–2802.

de Veubeke, B.F., 1965. Displacement and equilibrium models in the finite element method. In: Zienkiewicz, O.C., Holister, G.S. (Eds.), Stress Analysis. John Wiley and Sons.

Duff, I.S., Erisman, A.M., Reid, J.K. 1986. Direct Methods for Sparse Matrices. Oxford Science Publications.

Freitas, J.A.T., 1989. Duality and symmetry in mixed integral methods of elastostatics. Int. J. Numer. Meth. Engng 28, 1161–1179.

Freitas, J.A.T., 1997a. Formulation of elastostatic hybrid–Trefftz stress elements. Comp. Meth. Appl. Mech. Engng 153, 127–151.

Freitas, J.A.T., 1997b. Hybrid–Trefftz displacement and stress elements for elastodynamic analysis in the frequency domain. Comp. Assisted Mech. Engng Sci. 4, 345–368.

Freitas, J.A.T., Castro, L.M.S.S., 1997. Finite element solutions with Walsh series and Wavelets. Comp. Assisted Mech. Engng Sci. 4, 127–155.

Freitas, J.A.T., Almeida, J.P.M., Pereira, E.M.B., 1996. Non-conventional formulations for the finite element method. Int. J. Struct. Engng Mech. 4, 655–678.

Freitas, J.A.T., Cismasiu, C., Wang, Z.M., 1997. Comparative analysis of hybrid–Trefftz stress and displacement elements. Arch. Comput. Meth. Engng, in press.

Jirousek, J., Wróblewski, A., 1996. T-elements: state of the art and future trends. Arch. Comput. Meth. Engng 3, 323–434.

Maunder, E.A.W., Almeida, J.P.M., Ramsay, A.C.A., 1996. A general formulation of equilibrium macro-elements with control of spurious kinematic modes—the exorcism of an old curse. Int. J. Num. Meth. Engng 39, 3175–3194.

Munro, J., Smith, D.L., 1972. Linear programming duality in plastic analysis and synthesis. Int. Symp. Computer Aided Structural Design, Coventry.

NAFEMS, 1990. The Standard NAFEMS Benchmarks. Text FV32, Rev. 3, TNSB.

Papadrakakis, M., 1993. Solving large-scale linear problems in solid and structural mechanics. In: Papadrakakis, M. (Ed.), Solving Large-Scale Problems in Mechanics. John Wiley and Sons.

Pian, T.H.H., Tong, P., 1969. Basis of finite element methods for solid continua. Int. J. Num. Meth. Engng 1, 3–28.

Saad, Y., 1996. Iterative Methods for Sparse Linear Systems. PWS Publishing Company.